

TRACKING CONTROL FOR A FORMATION OF AUTONOMOUS UNDERWATER  
VEHICLES

by

John Gornowich  
A Thesis  
Submitted to the  
Graduate Faculty  
of  
George Mason University  
In Partial fulfillment of  
The Requirements for the Degree  
of  
Master of Science  
Electrical Engineering

Committee:



Dr. Gerald Cook, Thesis Director



Dr. Jill Nelson, Committee Member



Dr. Bernd-Peter Paris, Committee Member



Dr. Andre Manitius, Chairman, Department  
of Electrical and Computer Engineering



Dr. Lloyd J. Griffiths, Dean, The Volgenau  
School of Information Technology and  
Engineering

Date: 12/10/10

Fall Semester 2010  
George Mason University  
Fairfax, VA

Tracking control for a formation of Autonomous Underwater vehicles

A thesis submitted in partial fulfillment of the requirements for the degree of Master of Science at George Mason University

By

John Gornowich  
Bachelor of Science  
George Mason University, 2008

Director: Dr. Gerald Cook, Professor  
Department of Electrical and Computer Engineering

Fall Semester 2010  
George Mason University  
Fairfax, VA

Copyright: © 2010 by John Gornowich  
All Rights Reserved

## **DEDICATION**

This thesis is dedicated to my wife, Diane, and daughter, Cassidy, for the love and support they have given me through the course of this research. It was the prospect of our future together as a family that gave me the strength and motivation to see this through.

## ACKNOWLEDGEMENTS

I would like to thank my professor and thesis advisor, Dr. Gerald Cook, for all the support, guidance, and encouragement both technically and morally to see that this work was completed. We engaged in many profitable discussions throughout this process that helped maintain the road to success.

## TABLE OF CONTENTS

	Page
Abstract.....	x
1 Introduction.....	1
1.1 Background.....	1
1.2 Motivation.....	3
1.3 Problem Definition.....	4
1.4 Previous Work.....	6
1.5 Thesis Scope.....	8
1.6 Structure of Thesis.....	9
2 AUV Dynamics.....	11
2.1 REMUS Vehicle.....	11
2.2 Coordinate Frames.....	14
2.3 Equations of Motion.....	17
2.4 Model Simplification.....	24
2.5 Reduced Nonlinear Vehicle Model.....	24
3 Reference Trajectory a Heuristic Approach.....	27
3.1. Target Detection.....	27
3.2. Path Formulation.....	29
3.3. Path Tracking.....	32
4 Vehicle Control.....	36
4.1 REMUS Maneuvering Capabilities.....	36
4.2 Control Theory and Optimality.....	36
4.3 Linear Quadratic Tracker.....	37
4.4 Modified LQ Tracker.....	40

4.5	Basic Stability Check .....	41
4.6	Linearizing the Model for Tracking Problem .....	43
4.7	Weighting Matrix Comparison .....	46
4.8	Selected Control Summary .....	56
4.9	Numerical Integration Techniques.....	57
5	Cooperative Control.....	59
5.1	Search formation.....	61
5.2	Tracking formation .....	62
6	Simulation and Results .....	67
6.1	Introduction.....	67
6.2	Scenario 1.....	67
6.3	Scenario 2.....	72
6.4	Scenario 3.....	76
7	Conclusion .....	83
7.1	Thesis Summary.....	83
7.2	Research Conclusions .....	83
7.3	Proposed Future Research.....	84
	Appendices: A Matlab Code .....	85
A.1	Vehicle Dynamics .....	85
A.2	Numerical Integration.....	89
A.3	Feedback Control .....	90
	Bibliography .....	93

## LIST OF TABLES

Table	Page
Table 2.1 Basic Remus Vehicle Characteristics .....	13
Table 2.2 SNAME Motion Components for Marine Craft .....	16
Table 2.3 Equations of Motion Variable Descriptions .....	20
Table 2.4 Remus Hydrodynamic Coefficients .....	23
Table 4.1 Comparison of Weighting Matrices Q and R for LQ Tracker .....	49

## LIST OF FIGURES

Figure	Page
Figure 1.1 Typical Torpedo Shaped AUV .....	1
Figure 1.2 Different Underwater Vehicle Shapes.....	2
Figure 1.3 AUV Formation.....	5
Figure 2.1 REMUS AUV.....	12
Figure 2.2 Coordinate Frames and Euler Angles.....	15
Figure 2.3 Generic AUV Steering Model.....	26
Figure 3.1 Relative vs. True Target Bearing.....	28
Figure 3.2 High Level System Block Diagram.....	30
Figure 3.3 Over Simplified Path.....	31
Figure 3.4 Path Tracking Geometry.....	33
Figure 4.1 LQ Tracker Block Diagram.....	39
Figure 4.2 Basic LQ Feedback Block Diagram .....	41
Figure 4.3 Comparison of position and error on the x axis .....	50
Figure 4.4 Comparison of position and error on the y axis .....	50
Figure 4.5 Deviation from Target Tracking Distance.....	51
Figure 4.6 Comparison of Heading Error .....	53
Figure 4.7 Comparison of Required Thrust Input.....	54
Figure 4.8 Comparison of Required Rudder Input .....	55
Figure 5.1 Formation for Search Formation .....	62
Figure 5.2 Proposed Formation for Target Tracking.....	63
Figure 5.3 Information Flow Required for Reference Computation .....	64
Figure 6.1 XY Plot for Tracking a Target with Constant Heading.....	68
Figure 6.2 Zoomed in on Beginning of Tracking for Target with Constant Heading .....	68

Figure 6.3 Vehicle States for Tracking Target with Constant Heading.....	69
Figure 6.4 Control Inputs for Target Tracking with Constant Heading .....	69
Figure 6.5 Range Error from Reference for Target with Constant Heading .....	70
Figure 6.6 Tracking Range from Target with Constant Heading .....	70
Figure 6.7 Range Between Tracking Vehicles .....	71
Figure 6.8 XY Plot for Target Tracking with Offset Position .....	73
Figure 6.9 Vehicle States for Target Tracking with Offset Position .....	73
Figure 6.10 Control Inputs for Tracking Target with Offset Position .....	74
Figure 6.11 Range Error from Reference for Target with Offset Position .....	74
Figure 6.12 Tracking Range from Target with Offset Position .....	75
Figure 6.13 Range Between Tracking Vehicles .....	75
Figure 6.14 XY Plot for Tracking Target Through Heading Change.....	78
Figure 6.15 Zoomed in on End of Tracking Target Through Heading Change .....	78
Figure 6.16 Vehicle States While Tracking Target Through Heading Change .....	79
Figure 6.17 Control Inputs While Tracking Target Through Heading Change.....	79
Figure 6.18 Range Error from Reference Track for Target with Heading Change .....	80
Figure 6.19 Tracking Range form Target Through Heading Change.....	80
Figure 6.20 Range Between Tracking Vehicles .....	81

## **ABSTRACT**

### **TRACKING CONTROL FOR A FORMATION OF AUTONOMOUS UNDERWATER VEHICLES**

John Gornowich, M.S.

George Mason University, 2010

Thesis Director: Dr. Gerald Cook

Autonomous Underwater Vehicles (AUVs) are being implemented for a multitude of military and commercial applications, as well as scientific research and surveying. Because of the environment that these vehicles are tasked to perform duties in, there is a need for guidance and control schemes that are precise, yet robust. There are still major research efforts underway in the areas of system identification, modeling, control, and optimization to enhance the autonomy of these vehicles. This will allow for more advanced control schemes while maintaining the robustness that is required to operate in a diverse and hazardous environment such as the ocean.

Previous control algorithms for commercially available AUVs have been generally restricted to tracking straight-line trajectories between predetermined waypoints. These vehicles will typically employ an additional control technique that allows for obstacle determination and avoidance. Again, this is generally limited to a simple line of sight detection and preprogrammed avoidance maneuver. An even less

abundant and mature group of control schemes is available for a cooperative technique by a group of AUVs to accomplish a common goal.

This thesis addresses the development of a robust suboptimal tracking control algorithm that will efficiently and effectively track an identifiable target while maintaining a formation with cooperating vehicles. This work will examine the possibility of utilizing a common LTI control scheme for maneuvering the actual nonlinear vehicle model. It will also investigate a simple heuristic approach to determining how to track a given target, as well as in what formation to maintain the group structure.

## CHAPTER 1: Introduction

### 1.1. Background

Unmanned vehicles have become a key component in military as well as private industry applications. A class of unmanned vehicles that provide support in aquatic environments is the Unmanned Underwater Vehicle (UUV). Many of these vehicles are remotely driven by one or more operators via a tether that allows control signals and video feedback to be passed between the vehicle and the operator, as well as provide power. A special subclass of the UUV family is the Autonomous Underwater Vehicle (AUV), which can be preprogrammed before deployment and allowed to perform tasks without the constant direct interaction with an operator.



Figure 1.1 Typical Torpedo Shaped AUV (source: [www.asftauv.com](http://www.asftauv.com))

A brief history of AUV development as described by Blidberg [5] shows that AUV research can trace its beginnings back to the 1960's with theory and test bed applications. It was not until the 1980's and 1990's that experimental prototypes were developed and used for assessment of the technology. The advances in computing and design materials allowed AUV research and development to begin rapid expansion. However, it was not until the first part of the 2000's that the commercial market started to see its future potential in a variety of applications, and began offering packaged solutions. Figure 1.2 shows many of the shapes and sizes for which these solutions are still being be offered.



Figure 1.2 Different Underwater Vehicle Shapes (source: [www.rov-online.com](http://www.rov-online.com))

AUVs are currently being developed by several industries including educational institutions, government programs, and commercial companies for many different purposes. Increased intelligence and control for these vehicles is even more widely researched without respect to actual physical design of a new vehicle. Having autonomous vehicles that can work with minimal human interaction after deployment is a desirable technology that provides effectiveness in many underwater applications. With the current interest level of terrorism and anti-terrorism the military has a specific need for vehicles that can separate the mission from the risk to a soldier. Research institutions engaging in scientific surveying would benefit from advances in AUVs as these vehicles could dramatically expand the regions being searched, and therefore enhance the process of data acquisition.

## **1.2. Motivation**

The motivation for this research is driven by the author's interest in AUVs and their future roles in naval applications. This research is essential to gain an understanding of the technology at use in today's AUVs and to develop an essential platform for future work in this field of study. It is the author's intent to continue research within this field after the work contained herein is completed.

There is also a growing and sustainable need for AUVs in U.S. Naval applications. In the Navy's Mater Plan [5] it is stated that "UUV systems will provide a key undersea component" for future battle space. It continues to state, "The Navy needs stealthy and unmanned systems to gather information and engage targets in areas denied to traditional maritime forces." It is important to deploy such systems, but multiple

AUVs working together for a common goal is what will be needed to stay on the cutting edge.

The cooperation and coordination of multiple autonomous platforms performing independently to achieve a common goal is the future of AUV technology. Coordinating groups of AUVs could provide an advantage in many applications including those that would be accomplished less efficiently by a single vehicle.

### **1.3. Problem Definition**

There are many circumstances in which it becomes largely more efficient to deploy a group of unmanned vehicles that can coordinate activities in order to increase performance. A group of vehicles can cover more area in a search or surveying mission in the same amount of time than can an individual vehicle working alone. Coordinated groups of vehicles can also distribute the computational load required of detection and estimation of potential targets. Such systems can also benefit from increased mission success in hazardous environments like mine sweeping. If one vehicle becomes disabled while performing tasks, other vehicles in the group could quickly adjust to compensate the loss, rather than complete mission failure and restart, as would be the case with a single vehicle. It has also been theorized that a group of underwater vehicles may have more accurate results in determining their absolute position when they can sense each other.

This work will deal primarily with the scenario in which a formation of autonomous underwater vehicles is tasked with patrolling a given area of ocean for hostile target detection. Once a hostile craft has been detected, it is necessary to

maintain “eyes and ears” on the target until further action can be determined. This tracking can be done with an individual or sub-set of the searching group, while remaining vehicles continue patrolling. This problem can be realized in coastal protection, or port monitoring missions, where it is necessary to guard against unwanted vehicle presence that could be performing reconnaissance or attack an installation. For this work, it will be assumed that the entire group that is monitoring an area will remain together in tracking the target after detection has taken place.

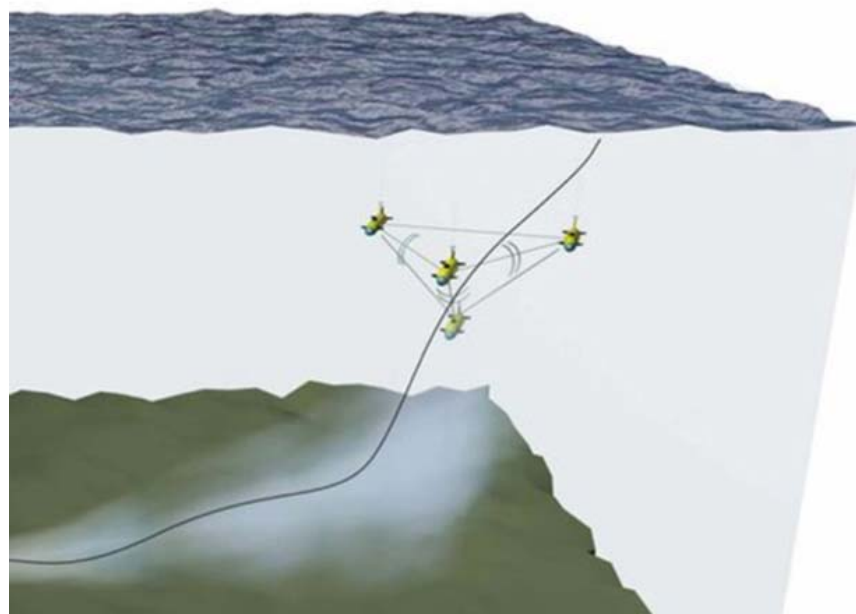


Figure 1.3 AUV Formation (source: [www.grex-project.eu](http://www.grex-project.eu))

This problem contains many individual components that must be solved in order to successfully achieve the desired coordination of these AUVs. This work would cover fields such as: guidance, navigation, communication, acoustic detection and estimation, as well as control theory. This thesis will primarily focus on the problems in guidance,

navigation, and control while making certain assumptions for the remaining fields of study that will help reduce the complexity of the entire work. It will also be assumed that the formation of the vehicles has been determined ahead of time, thus requiring the vehicles to only maintain their relative spacing rather than dynamically change such a formation during mission simulation.

It will be assumed for this work that the following technologies exist and can be included in an autonomous underwater vehicle:

- i. Inter vehicle communication can be achieved to allow each individual vehicle in the formation to receive and transmit information. The data transfer will be sufficient to relay vehicle position and orientation, as well as commands and other information required for target characteristics and tracking.
- ii. Detection of acoustic signatures that can initialize a tracking behavior by the coordinating group is available. This is important for the group transition from a monitoring phase to a tracking phase.
- iii. An algorithm exists such that each vehicle can acquire the target position and behavior continuously throughout the tracking portion of the mission.

#### **1.4. Previous Work**

The field of underwater vehicle development is unique and continuously growing. The research of control for these vehicles is a specific part of this field that contains some of the highest potential for advances. Autonomous control for robots is not a new idea, nor is it unfamiliar for an underwater vehicle platform. But the characteristics of the underwater environment make the control of vehicles there that much more challenging.

Because the water completely surrounds the vehicle, the main design consideration is typically focused on the effects that this medium will have on the slightest motions of the vehicle. It is also increasingly challenging in the fact that typical position updates for non-submerged vehicles is generated via GPS. However, GPS is not able to penetrate the water barrier for receipt beneath the surface. This requires a more complex method of determining a vehicles position without such a system. Typical advance methods use inertial navigation systems with complex estimation algorithms to accurately maintain knowledge of a vehicle's position and orientation.

Previous control algorithms for commercially available AUVs have generally been restricted to straight-line trajectories between predetermined waypoints, as described in Grabelle [8]. These vehicles will typically employ an additional control technique that allows for obstacle determination and avoidance, explained in Fodrea [3]. Again, this is generally limited to a simple Line of Sight (LOS) detection and preprogrammed avoidance maneuver.

There has been a great deal of research and model simulation into control techniques that will enhance the autonomy of underwater vehicles, allowing for more advanced control schemes while maintaining the robustness that is required to operate in such a diverse and hazardous environment as detailed in Repoulias and Papadopoulos [10]. A technique used to control formations of underwater vehicles has also been investigated in Okamoto [14]. Formation control of marine vehicles is also described in Børhaug [18], but this is more focused on the case where inter-vehicle communication is limited.

## **1.5. Thesis Scope**

The scope of this thesis is to utilize a previously developed AUV model and focus on advancing the robustness and capability of an algorithm for mission specific cooperative control. It is not the will of this thesis work to develop or redesign an actual underwater vehicle, but rather implement a different and potentially more effective control algorithm for a vehicle already widely in use. This work will maintain many of the assumptions that have been previously defined by other works, which will allow for more focus on the cooperative control algorithm, as well as tracking techniques.

As stated previously, this thesis will focus primarily on two areas. The first being the cooperation of multiple AUVs operating in a common area while maintaining some fundamental relative spacing that is required for formation of the vehicles. This will require simultaneous independent vehicle control simulations while maintaining a global view on what is happening to the group formation and overall objective. The second priority of this research will be for the group in formation to track a deterministic path that can vary over time based on some deterministic target trajectory.

One final simplification to this thesis development will be to disregard the vertical variability of the target and tracking vehicles. This simply means that any depth tracking maneuvering will be disregarded. Such a scenario can be found in the formational tracking of a surface vehicle by a group of underwater vehicles that are to maintain a constant depth or where depth is not critical to mission performance. The various unrelated vehicle control states, as well as environment uncertainties, will be kept to a minimum to help progress the work toward future research.

## **1.6. Structure of Thesis**

This research is intended to further enhance the control techniques for military and commercial application of AUVs in cooperative group formations. This is specifically directed toward the use of small, efficient, and expendable AUVs. This work will identify the type of vehicle to which the enclosed research is tailored, as well as the required control theory needed for a successful implementation. As stated in the problem definition of this research, it is essential for the tracking vehicles that are in formation to be able to share information to better determine, via acoustic detection algorithms, a target vehicle's position and trajectory.

Chapter 2 will show the development of the equations of motion that were used for vehicle simulation, specifically those for the REMUS vehicle. This section will also define the necessary coordinate frames required to relate measurable parameters from tracking vehicles to target position and orientation.

Chapter 3 will describe the geometry of commanding heading angle in relation to measureable sensor outputs in order to attain desired path following behavior.

Chapter 4 will provide some background on the control theory for this vehicle model, as well as outline the control algorithm that is developed for each vehicle in the formation used in this thesis research.

Chapter 5 will give details about multiple vehicle formations and cooperative control as it pertains to this research. This section will also show how the vehicles in formation behave in relation to one another.

Chapter 6 will provide a compilation of control simulation outputs generated for multiple scenarios to try to highlight the complete effectiveness of the control algorithm developed.

Chapter 7 will conclude this research effort with a brief summary and general conclusions that can be deduced from the work performed. This section will also contain suggestions on approach deficiencies and proposed future work.

## **CHAPTER 2: AUV Dynamics**

### **2.1. REMUS Vehicle**

The vehicle model chosen for the analysis and simulation of proposed control algorithms is the REMUS underwater vehicle. This specific underwater vehicle was chosen based on its proven history of performance, but more specifically because of the following:

- i. Vehicle parameters and hydrodynamic coefficients have been thoroughly characterized and tested by previous work done by T. Prestero [2].
- ii. The REMUS vehicle is used extensively by educational institutions for research and development in a variety of fields of study. It is also employed by the U.S. Navy for a variety of missions and has a history of success with the platform.
- iii. This vehicle also has a long list of previous works and experimental data to help fully understand its behavior in a real world environment. There seems to be more available previous research work for this platform than almost any other underwater vehicle sold commercially.

The REMUS AUV was developed by the Woods Hole Oceanographic Institute and is commercially supplied by Hydriod, Inc. There are three vehicles in this class, but

the two most applicable models being the 100 and 600. The REMUS 100 was designed for hydrographic reconnaissance up to 100 meters, while its larger variant the REMUS 600 was designed for greater payload support and up to 600 meters of operating depth. For increased efficiency, the REMUS 100 model has been used in all specifications and simulations in this thesis. Figure 2.4 below shows the vehicle out of the water, outfitted with upgraded modular components.

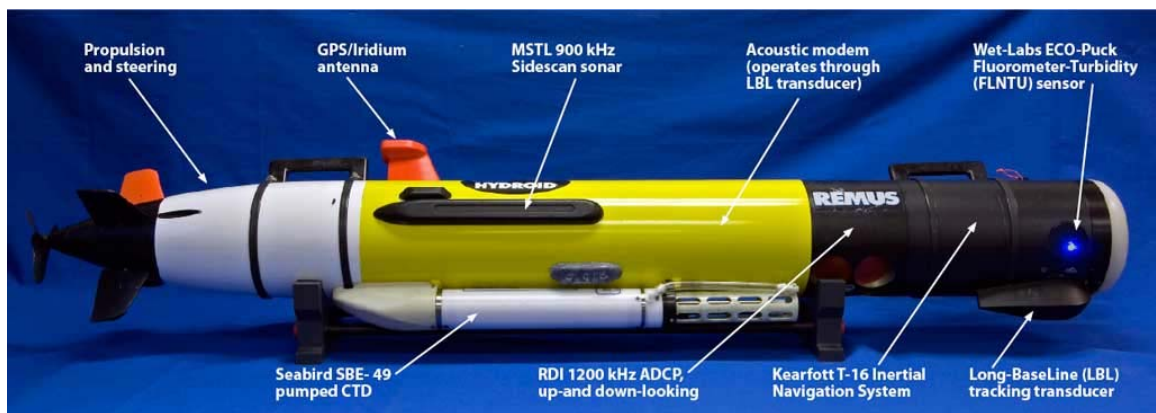


Figure 2.1 REMUS AUV (source: [www.whoi.edu](http://www.whoi.edu))

The REMUS 100 is a small, lightweight autonomous vehicle with proven reliability in both military and commercial domains. Weighing approximately 80 pounds, the REMUS 100 is an easy platform to launch and recover by a minimal team with limited equipment. This vehicle is available with a variety of payload options including an inertial navigation system, GPS, an acoustic modem, environmental sensors, and more. Its hull is shaped such that additional sensors could easily be adapted to this platform with minimal modifications as depicted in Figure 2.1.

The REMUS 100 is a battery driven vehicle that can provide endurance of more than eight hours on a single charge. Table 2.1 shows a more detailed view of some of the most common REMUS characteristics. These figures are just an approximation of general parameters for the vehicle that is outfitted in its most basic form without additional payload equipment. As expected, additional equipment would not only change the values of the baseline platform, but also have an effect on the more complex hydrodynamics that will be developed later in this chapter.

Table 2.1 Basic Remus Vehicle Characteristics

Characteristic	Symbol	Value	Units
Weight	W	2.99E+02	N
Buoyancy	B	3.06E+02	N
Length	L	1.33E+00	m
Diameter	D	1.91E-01	m
Max Speed	$U_{\max}$	2.88E+00	m / s
Max Depth	Z	1.00E+02	m

The propulsion of REMUS 100 includes a single propeller that can provide enough thrust to reach approximately five knots. The vehicle's control surfaces include four aft fins, two coupled in the horizontal position and two coupled in the vertical position. This allows commanded control of both pitch and yaw motions directly for maneuvering. At this point it should be fully stressed that the REMUS 100 vehicle, as is typical with most underwater vehicles, is an underactuated system. That is, the number of states that are directly controllable is less than the number of degrees of freedom of the

system. These types of systems can be increasingly challenging due to their typically complex hydrodynamic effects that should be dealt with by using the nonlinear model rather than a general linearized form.

## **2.2. Coordinate Frames**

The approach of this thesis is to treat the target trajectory-tracking problem as a path-following problem. The errors from the vehicle path to the desired path would then be taken into consideration and treated as a regulator problem. A coordinate system must be developed for this problem in order to relate the absolute position and orientation errors to local states variables that are capable of being controlled directly by the system. The two coordinate systems that will be defined are the:

- Earth-fixed coordinate frame
- Body-fixed coordinate frame

The earth-fixed coordinate frame takes its origin with respect to the globe. This earth-fixed frame is the same model used to describe the flat earth reference sometimes referred to as the north-east-down (NED) coordinate frame. However some minor modifications have been adapted from the standard NED model to fit this work's derivation better. For this thesis work, the origin is taken as some arbitrary point in the local area. This local origin and all subsequent points can then be converted to a more global set by a simple transformation based on the desired global origin. The body-fixed coordinate frame takes its origin at the gravitational center of the vehicle. It has been assumed here that the gravitational center of the vehicle is equal to the geometric center.

The Euler approach is used to obtain the transformation from one coordinate system to another, thus allowing for a link between the tracking errors and the vehicle states. Figure 2.2 shows how these two coordinate systems may relate to one another.

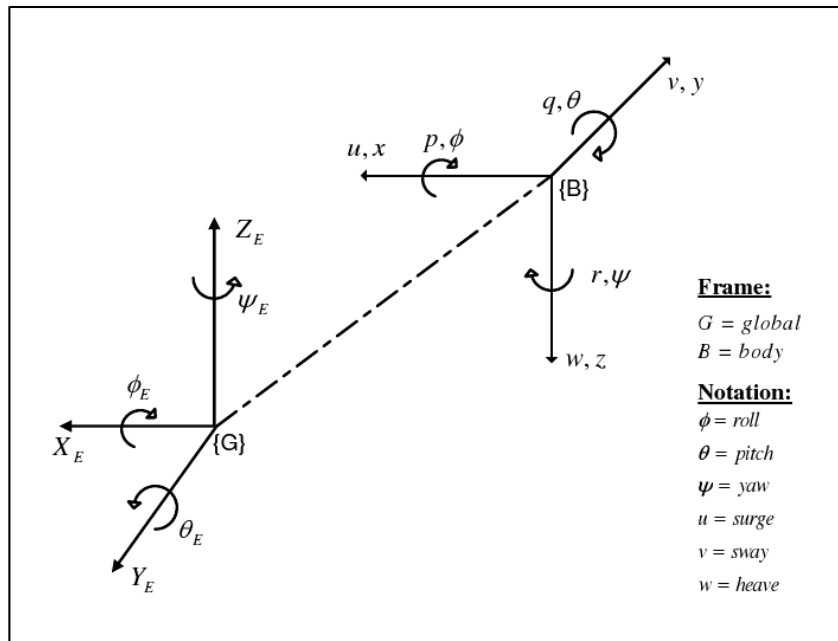


Figure 2.2 Coordinate Frames and Euler Angles

At this point a further explanation of the terminology that will be used for body fixed quantities is required. Surge is the term used to describe the velocity of the vehicle along the longitudinal axis. Similarly, sway is the term used to describe the lateral velocity of the vehicle. Lastly, heave is the term that defines velocity of the vehicle in the vertical direction. These terms have been summarized in Table 2.2.

Table 2.2 SNAME Motion Components for Marine Craft

Degree of Freedom	Name	Linear and Angular Velocity	Position and Euler Angles	External Forces
1	Surge	$u$	$x$	$X_f$
2	Sway	$v$	$y$	$Y_f$
3	Heave	$w$	$z$	$Z_f$
4	Roll	$p$	$\phi$	$K_f$
5	Pitch	$q$	$\theta$	$M_f$
6	Yaw	$r$	$\psi$	$N_f$

The body-fixed (local) velocities ‘ $u$ ’ (surge), ‘ $v$ ’ (sway), and ‘ $w$ ’ (heave) can be related to the earth-fixed (global) velocities ‘ $\dot{X}$ ’, ‘ $\dot{Y}$ ’, and ‘ $\dot{Z}$ ’ by defining a transformation matrix containing the Euler angles ( $\phi, \theta, \psi$ ). Equation 2.1 is a definition of the transformation matrix for such a relationship.

$$T(\phi, \theta, \psi) = \begin{bmatrix} \sin\psi\cos\theta & \sin\psi\cos\theta & -\sin\theta \\ \cos\psi\sin\theta\sin\phi - \sin\psi\cos\phi & \sin\psi\sin\theta\sin\phi + \cos\psi\cos\phi & \cos\theta\sin\phi \\ \cos\psi\sin\theta\cos\phi + \sin\psi\sin\phi & \sin\psi\sin\theta\cos\phi - \cos\psi\sin\phi & \cos\theta\cos\phi \end{bmatrix} \quad (5.1)$$

More formally:

$$\begin{bmatrix} \dot{X} \\ \dot{Y} \\ \dot{Z} \end{bmatrix} = T^{-1}(\phi, \theta, \psi) \begin{bmatrix} u \\ v \\ w \end{bmatrix} \quad (5.2)$$

Similarly, the body-fixed accelerations, ‘ $p$ ’ (roll rate), ‘ $q$ ’ (pitch rate), and ‘ $r$ ’ (yaw rate) can be related to the earth-fixed orientation rates by the transformation in equation 2.3.

$$\begin{bmatrix} \dot{\phi} \\ \dot{\theta} \\ \dot{\psi} \end{bmatrix} = \begin{bmatrix} 1 & \sin\phi \tan\theta & \cos\phi \tan\theta \\ 0 & \cos\phi & -\sin\phi \\ 0 & \frac{\sin\phi}{\cos\theta} & \frac{\cos\phi}{\cos\theta} \end{bmatrix} \begin{bmatrix} p \\ q \\ r \end{bmatrix} \quad (5.3)$$

However, an easy but very important simplification of this previous transformation is to assume that only small angular rotations, also known as the small angle theorem, are present and thus we can estimate the Euler angles with the following:

$$\dot{\phi} = p, \quad (5.4)$$

$$\dot{\theta} = q, \quad (5.5)$$

$$\dot{\psi} = r \quad (5.6)$$

This coordinate system model will be an important aspect of allowing the relationships to be built upon between the tracking vehicles and the environment in which the target is contained.

### 2.3. Equations of Motion

Now that we have defined the required transformations between the body-fixed and earth-fixed coordinate systems for the velocities, orientations, and positions, we can detail the equations of motion for this underwater vehicle. These equations of motion are adopted from work done originally by Healey [1] to derive this six-degree of freedom model. The technique used to derive these equations and relationships is founded on the Newton-Euler approach.

The following equations fully describe a vehicle's motion with six degrees of freedom, which include three translational and three rotational all in the body-fixed coordinate frame.

#### SURGE EQUATION OF MOTION

$$m[\dot{u} - vr + wq - x_G(q^2 + r^2) + y_G(pq - \dot{r}) + z_G(pq + \dot{q})] + (W - B)\sin\theta = X_f \quad (5.7)$$

#### SWAY EQUATION OF MOTION

$$m[\dot{v} + ur - wp + x_G(pq + \dot{r}) - y_G(p^2 + r^2) + z_G(qr - \dot{p})] - (W - B)\cos\theta\sin\phi = Y_f \quad (5.8)$$

#### HEAVE EQUATION OF MOTION

$$m[\dot{w} - uq + vp + x_G(pr - \dot{q}) + y_G(qr + \dot{p}) - z_G(p^2 + q^2)] + (W - B)\cos\theta\cos\phi = Z_f \quad (5.9)$$

#### ROLL EQUATION OF MOTION

$$\begin{aligned} I_x \dot{p} + (I_z - I_y)qr + I_{xy}(pr - \dot{q}) - I_{yz}(q^2 - r^2) - I_{xz}(pq + \dot{r}) \\ + m[y_G(\dot{w} - uq + vp) - z_G(\dot{v} + ur - w_r p)] \\ - (y_G W - y_B B)\cos\theta\cos\phi + (z_G W - z_B B)\cos\theta\sin\phi = K_f \end{aligned} \quad (5.10)$$

#### PITCH EQUATION OF MOTION

$$\begin{aligned} I_y \dot{q} + (I_z - I_x)pr - I_{xy}(qr + \dot{p}) + I_{yz}(pq - \dot{r}) + I_{xz}(p^2 - r^2) \\ - m[x_G(\dot{w} - uq + vp) - z_G(\dot{u} - vr + wq)] \\ + (x_G W - x_B B)\cos\theta\cos\phi + (z_G W - z_B B)\sin\theta = M_f \end{aligned} \quad (5.11)$$

### YAW EQUATION OF MOTION

$$\begin{aligned}
 I_z \dot{r} + (I_y - I_x)pq - I_{xy}(p^2 - q^2) - I_{yz}(pr + \dot{q}) + I_{xz}(qr - \dot{p}) \\
 + m[x_G(\dot{v} + ur - wp) - y_G(\dot{u} - vr + wq)] \\
 - (x_G W - x_B B)\cos\theta\sin\phi - (y_G W - y_B B)\sin\theta = N_f
 \end{aligned} \tag{5.12}$$

It must be recognized that the equations of motion that were derived previously require that the following three assumptions be maintained, as detailed by Healey [1]:

- i. The vehicle adheres to the behavior of a rigid body.
- ii. The rotation of the Earth can be neglected in effect on the vehicle accelerations.
- iii. The primary forces that act upon the vehicle are gravitation and inertial, which allows the forces due to the motion of the earth to be neglected.

There are some further assumptions that must be understood in order to apply these equations as well as to simplify them, which will be detailed in a later section of this chapter. I will briefly go through the necessary components that are required in order to arrive at the six equations that describe this vehicle motion according to Healey. The following table attempts to capture all of the variables used in the previous definition of the equations of motion.

Table 2.3 Equations of Motion Variable Descriptions

<b>Symbol</b>	<b>Name</b>	<b>Description</b>
W	weight	Weight of vehicle
B	buoyant force	Weight of water displaced by vehicle
m	mass	Mass of vehicle
g	gravitational force	Acceleration of gravity
V	volume	Volume of vehicle
A	area	Surface area of vehicle
$\rho$	density	Density of seawater
T	Transition matrix	Transition matrix from body fixed to earth fixed coordinates
x	x position	Position along the x axis
y	y position	Position along the y axis
z	z position	Position along the z axis
$\phi$	roll angle	Rotation about the x axis
$\theta$	pitch angle	Rotation about the y axis
$\psi$	yaw angle	Rotation about the z axis
u	surge	Translational velocity
v	sway	Lateral velocity
w	heave	Vertical velocity
p	roll rate	Angular velocity about the x axis
q	pitch rate	Angular velocity about the y axis
r	yaw rate	Angular velocity about the z axis
$X_f$		External forces applied along the x axis
$Y_f$		External forces applied along the y axis
$Z_f$		External forces applied along the z axis
$K_f$		Torque force applied along the x axis

<b>Symbol</b>	<b>Name</b>	<b>Description</b>
$M_f$		Torque force applied along the y axis
$N_f$		Torque force applied along the z axis
$x_G$	gravitational offset	Distance along the x axis from the vehicle center to the center of gravity
$y_G$	gravitational offset	Distance along the y axis from the vehicle center to the center of gravity
$z_G$	gravitational offset	Distance along the z axis from the vehicle center to the center of gravity
$x_B$	buoyancy offset	Distance along the x axis from the vehicle center to the center of buoyancy
$y_B$	buoyancy offset	Distance along the y axis from the vehicle center to the center of buoyancy
$z_B$	buoyancy offset	Distance along the z axis from the vehicle center to the center of buoyancy
$I_x$		Mass moment of inertia about the x axis
$I_y$		Mass moment of inertia about the y axis
$I_z$		Mass moment of inertia about the z axis
$I_{xy}$		Mass moment of inertial between the x and y axis
$I_{xz}$		Mass moment of inertial between the x and z axis
$I_{yz}$		Mass moment of inertial between the y and z axis

The external forces,  $X_f$ ,  $Y_f$ ,  $Z_f$ ,  $K_f$ ,  $M_f$ , and  $N_f$ , shown in the derivation of the equations of motion are also known as hydrodynamic coefficients. The precise values of these external forces have been previously addressed in the work by Prestero [2], and will

be summarized here for further understanding and completeness. The only external forces relevant to the steering model, and thus to the motion in the horizontal plan, are  $Y_f$ ,  $X_f$ , and  $N_f$ . They are expressed as the translational forces in surge and sway, as well as the rotational force in yaw are expanded by:

$$X_f = X_{u|u}|u|u| + X_{\dot{u}}\dot{u} + X_{vr}vr + X_{rr}r^2 + X_{prop} \quad (5.13)$$

$$Y_f = Y_{v|v}|v|v| + Y_{r|r}|r|r| + Y_{\dot{v}}\dot{v} + Y_{\dot{r}}\dot{r} + Y_{ur}ur + Y_{uv}uv + Y_{uu\delta_r}u^2\delta_r \quad (5.14)$$

$$N_f = N_{v|v}|v|v| + N_{r|r}|r|r| + N_{\dot{v}}\dot{v} + N_{\dot{r}}\dot{r} + N_{ur}ur + N_{uv}uv + N_{uu\delta_r}u^2\delta_r \quad (5.15)$$

We can see from equations 2.13 to 2.15 that there are two controls that can be utilized for motion control of coordinated maneuvers. The thrust input,  $X_{prop}$ , is directly proportional to the propeller torque applied via revolutions. And  $\delta_r$  is the rudder deflection angle of two coupled fins located in the stern of the vehicle.

The REMUS vehicle conforms to the Myring B hull shape, which describes a contour shape with minimal drag. This is an important characteristic in the derivation of the external forces that are acting upon the vehicle, as they are dependent primarily on the vehicle shape characteristics. Table 2.4 shows the actual values utilized in this work's model and simulation results; these values were originally presented in work by Prestero [2].

Table 2.4 Remus Hydrodynamic Coefficients

<b>Coefficient</b>	<b>Value</b>	<b>Units</b>	<b>Description</b>
$X_{u u }$	-1.62E+00	kg / m	Cross-flow drag
$X_{\dot{u}}$	-9.30E-01	kg	Added mass
$X_{vr}$	3.55E+01	kg / rag	Added mass cross-term
$X_{rr}$	-1.93E+00	kg * m / rad	Added mass cross-term
$Y_{v v }$	-1.31E+02	kg / m	Cross-flow drag
$Y_{r r }$	6.32E-01	kg * m / rad^2	Cross-flow drag
$Y_{\dot{v}}$	-3.55E+01	kg	Added mass
$Y_{\dot{r}}$	1.93E+00	kg * m / rad	Added mass
$Y_{ur}$	5.22E+00	kg / rad	Added mass cross-term & fin lift
$Y_{uv}$	-2.86E+01	kg / m	Body lift forces and fin lift
$Y_{uu\delta_r}$	9.64E+00	kg / (m * rad)	Fin lift force
$N_{v v }$	-3.18E+00	kg	Cross-flow drag
$N_{r r }$	-9.40E+00	kg * m^2 / rad^2	Cross-flow drag
$N_{\dot{v}}$	1.93E+00	kg * m	Added mass
$N_{\dot{r}}$	-4.88E+00	kg * m^2 / rad	Added mass
$N_{ur}$	-2.00E+00	kg * m / rad	Added mass cross-term & fin lift
$N_{uv}$	-2.40E+01	kg	Body and Fin Lift
$N_{uu\delta_r}$	-6.15E+00	kg / rad	Fin lift moment

$Y_{\delta}$  and  $N_{\delta}$  are the coefficient of forces and moments acting on the rudder control of the vehicle.

## 2.4. Model Simplification

The scope of this thesis research was reduced in that it ignores the motion of the vehicle in the vertical plane. This reduction eliminates the need to include the components  $w$ ,  $q$ , and  $Z$  in any of the equations 2.7 to 2.12. This simplification also means that the equations of motion for heave (eq 2.9), and pitch (eq 2.11), can be removed from this problem in their entirety. This is due to a nice theoretical fact that in the control development for this vehicle it can be assumed that the horizontal plane motion can be separated from the motion in the vertical plane. This means that for steering in a single plane only the dynamics of surge, sway, and yaw need be considered, thus reducing this six degree of freedom model down to just three degrees of freedom. When three dimensional vehicle control is required, the two sets of control surfaces can be stimulated simultaneously. This simplification does provide some important results, but one thing it does not provide is that the vehicle is no longer underactuated.

A final assumption that can be made, as previously addressed, to further simplify this set of nonlinear equations is that the geometric center is equal to the gravitational center, which is also equal to the center of buoyancy. That is:

$$x_G = y_G = z_G = 0 \quad (5.16)$$

$$x_B = y_B = z_B = 0 \quad (5.17)$$

## 2.5. Reduced Nonlinear Vehicle Model

The following is a summary of the simplified equations of motion that will be used in the remainder of this thesis work. This set of equations contains all the dynamics

that are required to simulate the nonlinear vehicle model in the horizontal steering plane. These equations can be broken into two parts, the first being the three-degree of freedom model for the vehicle:

$$(m - X_{\dot{u}})\dot{u} = X_{u|u}|u|u| + (X_{vr} + m)vr + X_{rr}r^2 + X_{prop} \quad (5.18)$$

$$(m - Y_{\dot{v}})\dot{v} - Y_{\dot{r}}\dot{r} = Y_{v|v}|v|v| + Y_{r|r}|r|r| + (Y_{ur} + m)ur + X_{uv}uv + Y_{uu\delta_r}u^2\delta_r \quad (5.19)$$

$$-N_{\dot{v}}\dot{v} + (I_{zz} - N_{\dot{r}})\dot{r} = N_{v|v}|v|v| + N_{r|r}|r|r| + N_{ur}ur + N_{uv}uv + N_{uu\delta_r}u^2\delta_r \quad (5.20)$$

The second part containing an augmented set of equations to include global position and orientation transformations.

$$\dot{X} = u \cos \psi - v \sin \psi \quad (5.21)$$

$$\dot{Y} = u \sin \psi + v \cos \psi \quad (5.22)$$

$$\dot{\psi} = r \quad (5.23)$$

Figure 2.3 shows the graphical representation of the nonlinear steering model described by equations 2.18 to 2.23.

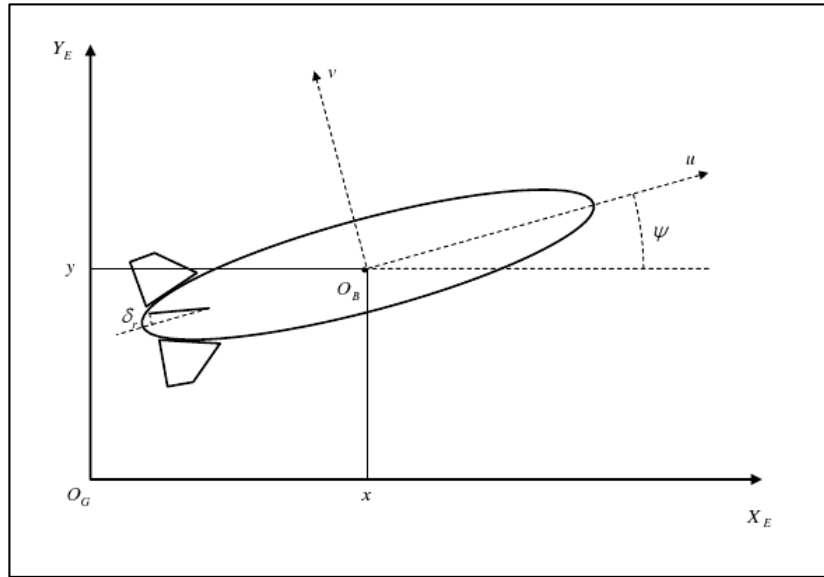


Figure 2.3 Generic AUV Steering Model

This figure for the AUV steering model provides a clear understanding of the parameters used, and their definition as far as what is said to be positive. All state quantities are measured in reference to the center of the body frame as depicted. One additional piece of information that can be seen in this figure is that positive rudder angle results in a positive heading angle. Positive rudder angle is defined as a deflection in the positive  $v$  direction, toward the port side of the vehicle.

## **CHAPTER 3: Reference Trajectory a Heuristic Approach**

The term “heuristic” refers to a problem solving approach that bases a solution on intuition and experience-based assumptions. This technique has been widely used in mobile robots for path planning, as well as obstacle avoidance, and has a past performance for providing adequate solutions depending on the problem tasks. These types of approaches prefer to develop a solution that provides good realistic performance that may be sub optimal to other more extensive methods. In many cases there is no way to mathematically prove that the method developed is a near optimal solution. Instead the solution can only be evaluated on its ability to perform a task as directed, and measure some performance characteristics to compare to a given set of metrics.

### **3.1. Target Detection**

This thesis problem deals with the path tracking of a target by a group of AUVs; because of this, an understanding of the track determination must be fully understood. This section will detail the required geometric principles and relationships that allow the proper reference command to be calculated in order for the vehicle controller to perform properly. These fundamentals can be evolved from the basics of target motion analysis that is common with underwater vehicles, most notably submarines. Target motion analysis is a large and complicated field of study not only in marine applications. These techniques are all built upon some basic trigonometric rules. A brief description of

important quantities from this analysis technique, including bearing and range, will be shown as it is important to determining the required path for the tracking AUV to follow and remain on.

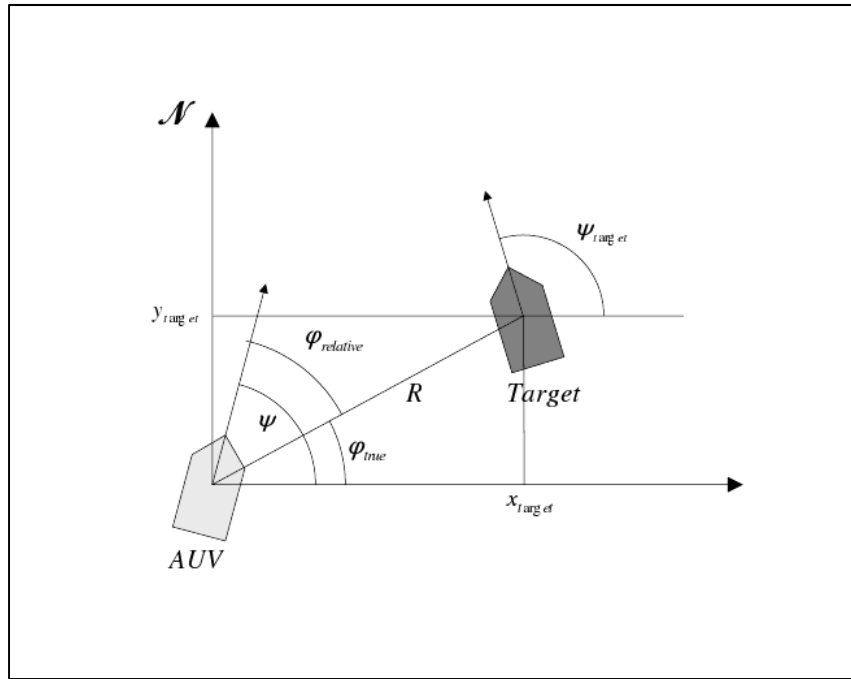


Figure 3.1 Relative vs. True Target Bearing

There are many active and passive sonar systems that can perform an analysis of acoustic signatures to determine range and relative bearing of a target source from a vehicle's current position. It will be understood that such a system exists and it is not the requirement of this thesis work to develop such algorithms. Instead it will be assumed that this information is available to each tracking vehicle in these simulations for use in determination of a tracking path. Figure 3.1 shows the relationship between relative and true target bearing between a vehicle and the target once detection has been established. Typical algorithms that perform such detection tasks here can typically only estimate a

target position relative to its own location; that is, all computed quantities take their origin from the center of the tracking vehicle. This requires that a few computations be made in order to transform target vehicle characteristics into the same reference frame as the tracking vehicle.

Relative bearing is defined to be the angle formed by the LOS segment between the two vehicles and the direction of course of the tracking vehicle. This relationship is expressed by:

$$\varphi_{true} = \psi - \varphi_{relative} \quad (6.1)$$

Earth-fixed position of the target can then be computed by the following relationship that uses the tracking vehicles position and the detectable range of the target vehicle.

$$x_{target_{true}} = x + R \cos(\varphi_{true}) \quad (6.2)$$

$$y_{target_{true}} = y + R \sin(\varphi_{true}) \quad (6.3)$$

### **3.2. Path Formulation**

This thesis work will require the use of two distinct motion tasks, path following and trajectory tracking. The trajectory tracking of this problem will be achieved by computation from known target position and orientation, which were derived in equations 3.2 and 3.3. This computation will include all desired tracking characteristics such as tracking distance, heading error, and positioning. This computation will resolve the desired reference command that will be passed to a vehicle controller, shown in Figure

3.2 as the “innerLoop,” to reduce the total solution to a path-tracking problem. This figure also depicts an “outerLoop” in which the reference commands, as well as vehicle states will be assumed to be transmitted via acoustic communication channels among vehicles in the group formation or other base stations.

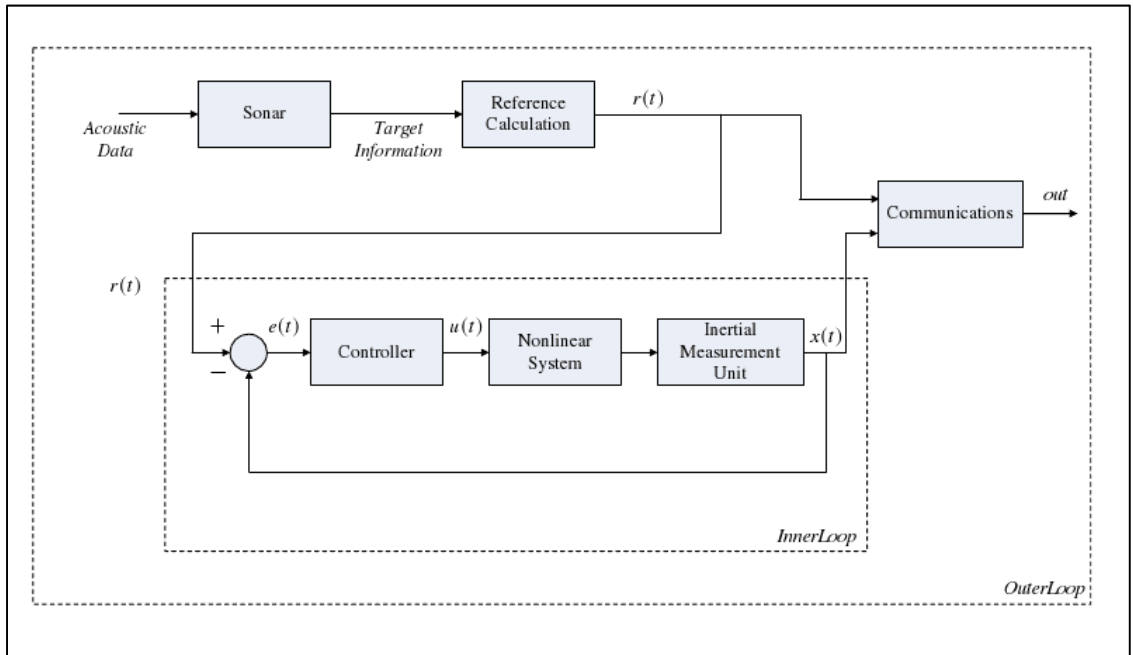


Figure 3.2 High Level System Block Diagram

Figure 3.3 shows a simple way to determine a path to track based on a target path and required tracking distance. Which is expressed by:

$$\dot{x}_{path} = x_{target} - L \cos(\psi_{target}) \quad (6.4)$$

$$\dot{y}_{path} = y_{target} - L \sin(\psi_{target}) \quad (6.5)$$

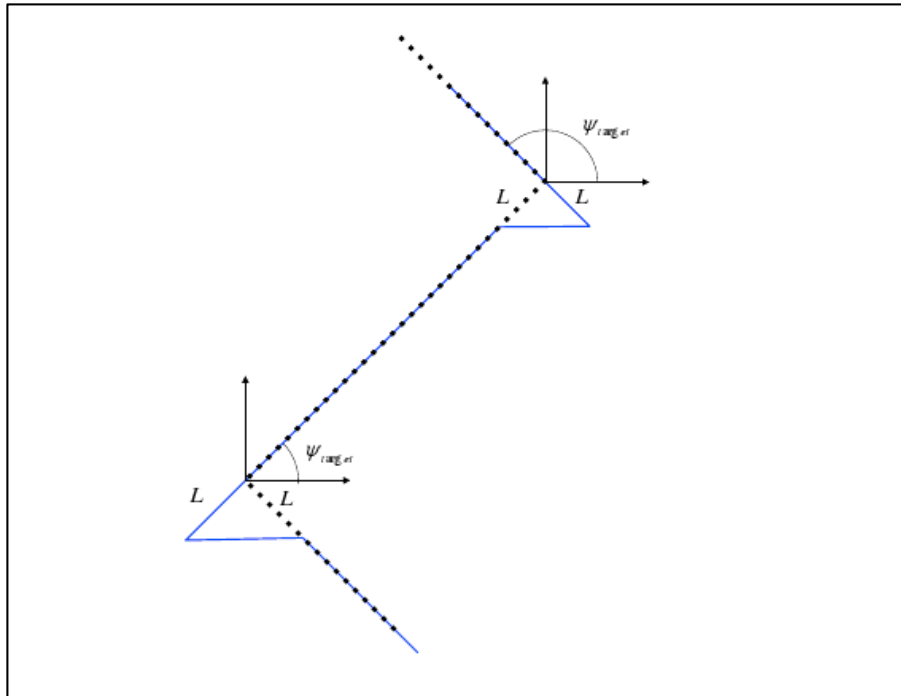


Figure 3.3 Over Simplified Path

This type of path is not actually capable of being tracked by a marine vehicle because of two reasons. One being that there is a obvious discontinuity when the target vehicle heading is changed abruptly. The second being that it is not common practice for a marine vehicle, especially an underwater vehicle, to possess the capabilities that are required to make a sudden changed in direction equal to or greater than a ninety degree angle. Because of this, a “smoother” path must be determined for the tracking vehicle to follow. Such a path can be generated using equations 3.6 and 3.7.

$$\dot{x}_{path} = x_{target} - L \cos\left(\text{atan}\left(\frac{y_{target} - y_{path}}{x_{target} - x_{path}}\right)\right) \quad (6.6)$$

$$\dot{y}_{path} = y_{target} - L \sin\left(\text{atan}\left(\frac{y_{target} - y_{path}}{x_{target} - x_{path}}\right)\right) \quad (6.7)$$

where “L” is the desired distance between the target and the lead tracking vehicle.

### 3.3. Path Tracking

The controller designed in this thesis will focus on following the generated reference path and compensate for any initial off path errors. This initial error between the tracking vehicle position and the computed reference path must not be too dramatic or an undesirable erratic behavior may manifest itself. However, this should not be of significance to this thesis work, as it is assumed that the desired reference path is computed only once a target is sufficiently close that it can be detected.

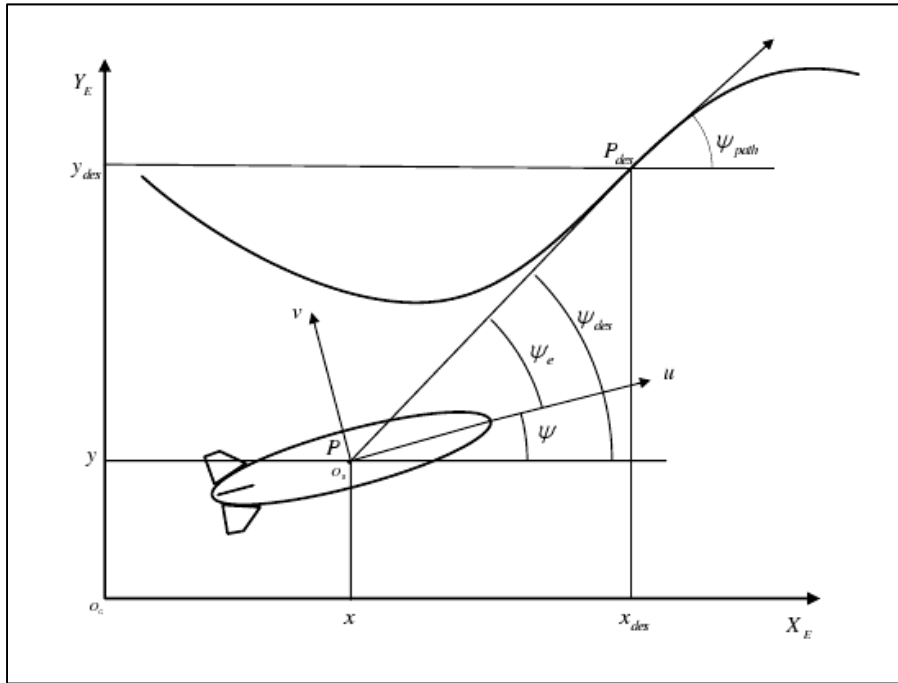


Figure 3.4 Path Tracking Geometry

Figure 3.4 shows the geometry of a tracking vehicle in relation to the computed reference trajectory that is to be used for path following. The position error between the actual tracking vehicle position and the reference path at a given time is found by:

$$x_{error} = x_{des} - x \quad (6.8)$$

$$y_{error} = y_{des} - y \quad (6.9)$$

The error in commanded heading and the heading of the target vehicle at the same point in space is found by:

$$\psi_{error} = \psi_{des} - \psi \quad (6.10)$$

The straight-line distance between the current position of the tracking AUV and the desired reference path is found by:

$$range_{error} = \sqrt{x_{error}^2 + y_{error}^2} \quad (6.11)$$

It will also be assumed that a significant enough inertial measurement unit is available onboard each vehicle that can precisely measure local position and orientation to accurately determine current location in relation to the reference path. Such a system allows for accurate construction of the vehicle's global position and orientation, as well as vehicle translational and angular velocities. It is also known that this vehicle is underactuated and does not allow for direct control of motion in the sway direction that can add to the complications of reliable control. Because of this the AUVs can only maintain on track by control through both the rudder deflection and the thrust applied for propulsion.

We can see from figure 3.4 that the major problem that must be undertaken is the compensation of the error off path. This error is also known as the Cross Track Error (CTE) of a tracking vehicle in relation to a given path that should be followed. The starting point of the commanded reference in terms of heading angle to track is only an initial piece of the problem. Some computations must be used to determine the heading angle that is required to remove this CTE that is inherent in the underwater target tracking that has been set forth in this thesis work. Rather than using a reference heading of the target vehicle, the commanded heading for the tracking AUV is given by:

$$\psi_{des} = \text{atan}\left(\frac{y_{error}}{x_{error}}\right) \quad (6.12)$$

It will be shown in Chapter 5 that the computation for the desired heading angle for any given AUV in the formation can be expanded to include not only characteristics of the target, but also additional AUVs in the group formation.

## **CHAPTER 4: Vehicle Control**

### **4.1. REMUS Maneuvering Capabilities**

As previously stated, the REMUS vehicle is limited to four total control surfaces in the stern of the vehicle. These four control surfaces are controlled in pairs, with two capable of yaw motion adjustment and two capable of inducing changes in pitch motion. A single rear propeller provided thrust for forward movement of the vehicle. For this thesis work we will only be interested in controlling the two fin surfaces that can manipulate the yaw angle of the vehicle. We have removed the cross coupling terms in the derivation of the equations of motion from Chapter 2 that would require control of the other two stern planes that affect pitch motion.

### **4.2. Control Theory and Optimality**

Control of an AUV is uniquely difficult due to the underactuation of the vehicle relative to the degrees of freedom in which it can be maneuvered. Another difficult challenge for this type of vehicle is the ocean environment in which it is designed to operate. The underwater environment is unlike any other on this planet in that the outside forces acting as disturbances on the vehicle can change dramatically in just a few meters in any of the three directions. Even the slightest external disturbance can induce a large magnitude of error in the system. The medium of water can be much more demanding to

traverse than air, and underwater vehicles are limited by the power in which it can carry on board. Because of this, it is essential to take into consideration the power that will be expended controlling the vehicle and weigh tradeoffs between accuracy and endurance in some circumstances.

Optimal control focuses on the determining of an input sequence that will deliver the desired output response given some specific performance requirements and possibly some system constraints. System constraints are commonly applied to limit the problem based on more real world criteria such as maximum thrust or minimum turning radius. It is important to determine the desired performance that the system should implement before designing a controller. Typical performance metrics can be described by the following generalized cost functions:

$$J = \int_{t_0}^T 1 dt \quad (\text{Minimum Time})$$

$$J = \int_{t_0}^T |u(t)| dt \quad (\text{Minimum Fuel})$$

$$J = \frac{1}{2} \int_{t_0}^T [x^T(t)Qx(t) + u^T(t)Ru(t)] dt \quad (\text{Minimum Quadratic Error})$$

### 4.3. Linear Quadratic Tracker

The specific control structure for this thesis work is developed using the output feedback Linear Quadratic (LQ) tracker. The cost function for this control approach is similar to the minimum quadratic error cost. This technique was chosen for its robustness, as well as its ability to clearly determine a performance metric initially and allow this to propagate through the controller design. This approach can often lead to more desirable designs than the tuning that is required with more classical control design,

such as PID, to minimize error in final output. However, it is shown later in this chapter that because the vehicle is highly nonlinear, a direct linear control method may not be sufficient to implement without some modifications.

In order to expand on the control design procedure, some detail in the fundamentals of the optimal output feedback LQ tracker will be discussed here. The linear quadratic tracking problem is based on the LQ regulator problem, but instead of regulating the states to near zero value it is desired to follow some non-zero reference input command. The traditional formulation of the LQ problem for a continuous time system as detailed by Lewis [12], is to define a system as:

$$\dot{x} = f(x, u) \quad (7.1)$$

$$y = Cx(t) \quad (7.2)$$

With a quadratic cost index to keep the system states close to a predetermined reference track given by:

$$J(t_0) = \frac{1}{2}(Cx(T) - r(T))^T P(Cx(T) - r(T)) + \frac{1}{2} \int_{t_0}^T [(Cx - r)^T Q(Cx - r) + u^T R u] dt \quad (7.3)$$

where  $P \geq 0$ ,  $Q = 0$ , and  $R > 0$ .

After some derivation [12] represents the optimal affine control solution from:

$$K(t) = R^{-1} B^T S(t) \quad (7.4)$$

$$-\dot{S} = A^T S + SA - SBR^{-1}B^T S + C^T QC, \quad S(T) = C^T PC \quad (7.5)$$

$$-\dot{v} = (A - BK)^T v + C^T Qr, \quad v(T) = C^T Pr(T) \quad (7.6)$$

$$u = -Kx + R^{-1}B^T v \quad (7.7)$$

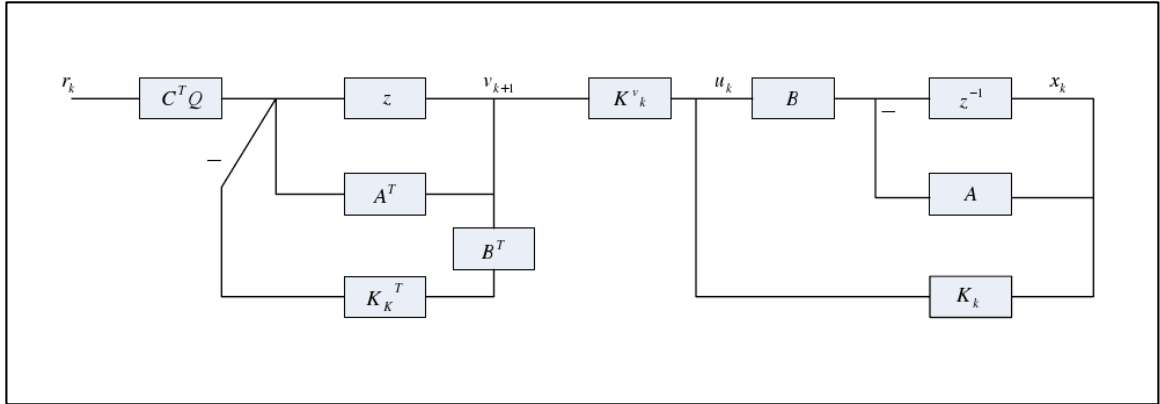


Figure 4.1 LQ Tracker Block Diagram

The control gains for this LQ tracker problem can be determined offline by solving the Algebraic Riccati Equations (ARE) backward in time. It should be noted that the optimal LQ tracker that has been described in this section is not a causal system. This is because the future reference input sequence must be known for computation of the system input signal. Instead, for simulation of this thesis work, a suboptimal estimate of the solution will be used to allow for an on-line control structure that can be implemented. While this step will cause the solution to become sub-optimal it does allow for a realistic implementation for this control design.

#### 4.4. Modified LQ Tracker

Because this optimal LQ tracker from the previous section cannot be implemented due to causality issues, a modified solution will be introduced. This technique requires the use of both feedforward and feedback terms that are not typical in the traditional formulation of the tracker problem. First a definition of the system to be used must be defined.

$$\dot{x} = Ax + Bu + Gr \quad (7.8)$$

$$y = Cx + Fr \quad (7.9)$$

Then the control input will take the form:

$$u = -Ky = -KCx - KFr \quad (7.10)$$

The closed-loop system will thus take the form:

$$\dot{x} = (A - BKC)x + (G - BKF)r \quad (7.11)$$

Now the problem that remains is the selecting of  $K$  that will control the system to track an desired reference input. This method is typically done using software like MATLAB's `lqr.m` function for its steady-state solution. However, it will be shown analytically how these gains, and thus the optimal linear control, may be computed by solving the following ARE:

$$K = R^{-1}B^T P \quad (7.12)$$

$$-\dot{P} = A^T P + PA + Q - PBR^{-1}B^T P \quad (7.13)$$

Where the steady-state solution can be found when  $\dot{P} = 0$ .

A quadratic performance index that should be minimized is defined by:

$$J = \frac{1}{2}x^T(T)S_Tx(T) + \frac{1}{2}\int_{t_0}^T [x^T(t)Qx(t) + u^T(t)Ru(t)]dt \quad (7.14)$$

where:  $S_T > 0$ ,  $Q \geq 0$ ,  $R > 0$  are the design parameters that may be chosen to satisfy a given system response.

We can see this graphically in the following general LQ tracker block diagram:

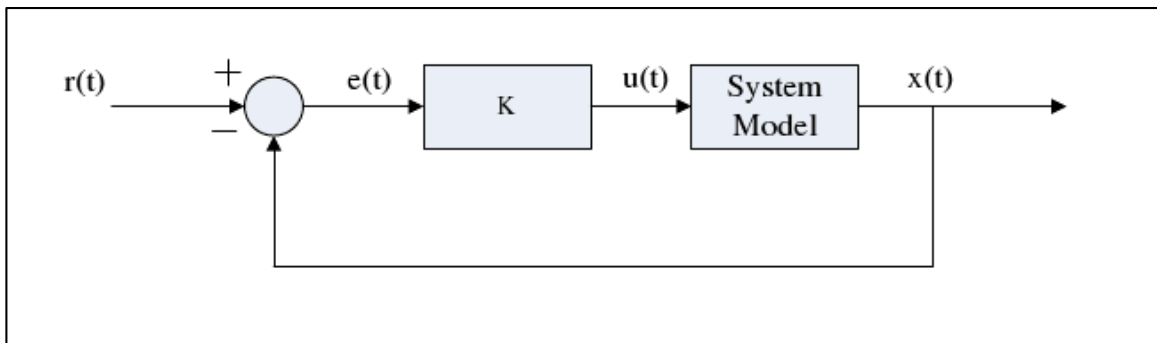


Figure 4.2 Basic LQ Feedback Block Diagram

#### 4.5. Basic Stability Check

The LQ tracker in the theoretical derivation is meant to provide a solution of feedback gains such that the system maintains stability. However, if the steady-state gain is used over some finite interval of control in order to simplify computational requirements, stability is not as strictly formulated. While this steady state gain feedback may be used and provide satisfactory results, the absolute stability of the system cannot be guaranteed. Necessary conditions for closed-loop stability are guaranteed if the system is detectable and stabilizable. However, two more simple conditions that are sufficient and more easily tested are observability and controllability of the system.

An initial intuitive check to whether this is a reasonable set of gains that can be utilized is to check the rank of the system controllability matrix. The controllability matrix can be formed by:

$$C = [B \quad AB \quad A^{n-1}B] \quad (7.15)$$

This controllability matrix can only contain full rank if the controllability Gramian is nonsingular for every  $t > 0$ . The controllability Gramian is given by:

$$W_c(t) = \int_0^t e^{-A\tau} B^T B e^{-A^T \tau} d\tau \quad (7.16)$$

The second sufficient test is for observability of the system, regarding whether all components of the state impact the performance measure. This observability matrix can be constructed from the system by:

$$O = \begin{bmatrix} C \\ CA \\ \vdots \\ CA^{n-1} \end{bmatrix} \quad (7.17)$$

where:  $C = \sqrt{Q}$

This observability matrix can only contain full rank if the observability Gramian is nonsingular for every  $t > 0$ . This observability Gramian is given by:

$$W_o(t) = \int_0^t e^{A^T \tau} C^T C e^{A\tau} d\tau \quad (7.18)$$

This observability condition restricts the choices for the weighting matrices, but provides for the fact that all states are weighted in the performance criterion either directly or indirectly. If both the observability and controllability matrices contain full rank and the R matrix is positive definite then it can be said that the vehicle's linearized system model is stable for the specified weighting matrices and feedback gains. However, an important note here is that just because the stability of the linearized system can be satisfied, it is not guaranteed that this same feedback solution will result in a stable nonlinear system. Instead, it can only be said that this is the best solution that exists given the system and technique at hand.

#### **4.6. Linearizing the Model for Tracking Problem**

Feedback control gains will be based on the LQ tracker design, but the steady-state gain matrix will be utilized at all instances in time for the simulation. The steady-state quadratic tracker gain will be determined based on the system linearization. This linearization is performed when the AUV is in a typical straight-line motion.

The previous sections have described how the REMUS vehicle used in this thesis can be controlled, as well as some background on the control technique that will be utilized. As noticed in the derivation of the equations of motion, even the reduced model remains highly nonlinear and thus cannot be controlled by a typical linear time invariant technique directly. Instead the LQ tracking problem will be adapted to the nonlinear system by first linearizing the system relative to a subset of current state values. This will allow for the control gains to be determined by solving the LQ tracker problem at an equilibrium. This method of linearizing the system at a given point in time with actual

state values will provide a reasonable result for the trajectory tracking laid out in the problem definition of the thesis.

Using the reduced nonlinear model equations in Chapter 2, the linearized system dynamics can be assumed to take on the following state space form:

$$\dot{x} = Ax + Bu + W \quad (7.19)$$

Where “W” represents any disturbances to the system, which for this thesis work will be assumed to be negligible.

The system state vector will take on the form:

$$x = [u \quad v \quad r \quad X \quad Y \quad \psi]^T \quad (7.20)$$

The control input will take on the generalized form:

$$u = -K^T x_{error} \quad (7.21)$$

Where “u” can be expanded knowing that “K” is the steady-state gain feedback matrix to be designed by this process:

$$u = \begin{bmatrix} k_{11} & k_{12} & k_{13} & k_{14} & k_{15} & k_{16} \\ k_{21} & k_{22} & k_{23} & k_{24} & k_{25} & k_{26} \end{bmatrix} \begin{bmatrix} u_{error} \\ v_{error} \\ r_{error} \\ X_{error} \\ Y_{error} \\ \psi_{error} \end{bmatrix} \quad (7.22)$$

However, there is a specific sub-set of the previously defined control gains that can be neglected due to their indirect inclusion in other control input commands. It has been seen through experience that the inclusion of these gains can at times apply too much control, causing adverse effects to the system. Therefore, the following control gains can be removed:

$$k_{23} = k_{24} = k_{25} = 0 \quad (7.23)$$

This system model will utilize full state feedback and thus no output equation will be shown in the state space representation.

To determine a linearization for the state space representation, the reduced nonlinear model equations will be differentiated with respect to each of the state variables. This model will then be evaluated at some equilibrium point of the vehicle, using actual state values for any of the parameters that are required. This process can be visualized by the following symbolic representation of A and B at any given instance in time.

A

$$= \begin{bmatrix} \frac{a_{11}}{m_{11}} & \frac{a_{12}}{m_{11}} & \frac{a_{13}}{m_{11}} & 0 & 0 & 0 \\ \frac{a_{21}m_{33} - a_{31}m_{23}}{m_{22}m_{33} - m_{23}m_{32}} & \frac{a_{22}m_{33} - a_{32}m_{23}}{m_{22}m_{33} - m_{23}m_{32}} & \frac{a_{23}m_{33} - a_{33}m_{23}}{m_{22}m_{33} - m_{23}m_{32}} & 0 & 0 & 0 \\ \frac{a_{31}m_{22} - a_{21}m_{32}}{m_{22}m_{33} - m_{23}m_{32}} & \frac{a_{32}m_{22} - a_{22}m_{32}}{m_{22}m_{33} - m_{23}m_{32}} & \frac{a_{33}m_{22} - a_{23}m_{32}}{m_{22}m_{33} - m_{23}m_{32}} & 0 & 0 & 0 \\ \cos(\psi(ii)) & -\sin(\psi(ii)) & 0 & 0 & 0 & -u(ii)\sin(\psi(ii)) - v(ii)\cos(\psi(ii)) \\ \sin(\psi(ii)) & \cos(\psi(ii)) & 0 & 0 & 0 & u(ii)\cos(\psi(ii)) - v(ii)\sin(\psi(ii)) \\ 0 & 0 & 1 & 0 & 0 & 0 \end{bmatrix} \quad (7.24)$$

With the required coefficients being defined as:

$$a_{11} = 2X_{u|u}|u(ii)|$$

$$a_{12} = (X_{vr} + m)r(ii)$$

$$a_{13} = (X_{vr} + m)v(ii) + 2X_{rr}r(ii)$$

$$a_{21} = (Y_{ur} - m)r(ii) + Y_{uv}v(ii)$$

$$a_{22} = 2Y_{vv}|v(ii)| + Y_{uv}u(ii)$$

$$a_{23} = 2Y_{rr}|r(ii)| + (Y_{ur} - m)u(ii)$$

$$a_{31} = N_{ur}r(ii) + N_{uv}v(ii)$$

$$a_{32} = 2N_{vv}|v(ii)| + N_{uv}u(ii)$$

$$a_{32} = 2N_{rr}|r(ii)| + N_{ur}u(ii)$$

$$m_{11} = (m - X_{\dot{u}})$$

$$m_{22} = (m - Y_{\dot{v}})$$

$$m_{23} = -Y_{\dot{r}}$$

$$m_{32} = -N_{\dot{v}}$$

$$m_{33} = (I_{zz} - N_{\dot{r}})$$

$$B = \begin{bmatrix} \frac{1}{(m - X_{\dot{u}})} & 0 \\ 0 & \frac{2u(ii)[N_{uu\delta_r}Y_{\dot{r}} + Y_{uu\delta_r}(I_{zz} - N_{\dot{r}})]}{(m - Y_{\dot{v}})(I_{zz} - N_{\dot{r}}) - Y_{\dot{r}}N_{\dot{v}}} \\ 0 & \frac{2u(ii)[N_{uu\delta_r}(m - Y_{\dot{v}}) + Y_{uu\delta_r}N_{\dot{v}}]}{(m - Y_{\dot{v}})(I_{zz} - N_{\dot{r}}) - Y_{\dot{r}}N_{\dot{v}}} \\ 0 & 0 \\ 0 & 0 \\ 0 & 0 \end{bmatrix} \quad (7.25)$$

#### 4.7. Weighting Matrix Comparison

The performance metric that is defined through the selection of the Q and R matrices has a direct relationship with the response times and robustness of the system. Selection of the elements of Q and R are typically done in such a way that these weighting matrices are diagonal. This tuning of the LQ tracker performance does involve a somewhat trial and error approach. However, there are methods that have been developed in order to aid

in this selection including works by Bryson [22] that have been briefly touched on in Lewis [12].

Q is the weighting matrix containing the relative importance of each of the system states. As a general rule, increasing the weighting on one of these parameters will limit the allowable control effort applied due to this state. The Q matrix for this problem can be expanded by:

$$Q = \text{diag}\{q_u, q_v, q_r, q_x, q_y, q_\psi\} \quad (7.26)$$

It is shown in the previous section that due to the coupling of the system model that the first three states,  $u$ ,  $v$ , and  $r$  are going to be incorporated in the weight given to the final three states. Therefore, it is for this reason, that the majority of the weighting matrix comparisons have no direct weight on these states. By placing no weight on these states, it is implied that there is no requirement to maintain them about some specified value.

R is the relative important weight of the allowed input controls on the system. The two control inputs that can be weighted are the propeller thrust and the rudder deflection angle.

$$R = \begin{bmatrix} r_{11} & r_{12} \\ r_{21} & r_{22} \end{bmatrix} = \text{diag}\{r_{prop}, r_{rudder}\} \quad (7.27)$$

The available range of these two inputs must be understood before trying to take on a selection of  $r_{prop}$  and  $r_{rudder}$ .

The maximum value of thrust is found by:

$$u_{max} = c * v_{max}^2 \quad (7.28)$$

Where the constant c was determined by:

$$c = \frac{u_{max}}{v_{max}^2} = \frac{19.845}{5^2} = 0.7938 \quad (7.29)$$

The maximum value of  $u$ , was determined by experimental methods of requiring the system to track a significantly large input, and determining where the limits of the vehicle model were induced.

The maximum rudder deflection angle was taken to be:

$$\delta_{r\_max} = 15^\circ = 0.2618 \text{ radians} \quad (7.30)$$

Because of the unit magnitude difference in the two control inputs, the following ratio is advisable:

$$\frac{r_{11}}{r_{22}} \approx 100 \quad (7.31)$$

Several different design selections for these Q and R matrices were evaluated in order to make the best possible selection in terms of performance tradeoffs, and have been compiled in Table 4.1

Table 4.1 Comparison of Weighting Matrices Q and R for LQ Tracker

Trial	Q	R	X (m)	Y (m)	Range (m)	Heading (r)
1	$\begin{bmatrix} \mathbf{1} & 0 & 0 & 0 & 0 & 0 \\ 0 & \mathbf{1} & 0 & 0 & 0 & 0 \\ 0 & 0 & \mathbf{1} & 0 & 0 & 0 \\ 0 & 0 & 0 & \mathbf{1} & 0 & 0 \\ 0 & 0 & 0 & 0 & \mathbf{1} & 0 \\ 0 & 0 & 0 & 0 & 0 & \mathbf{1} \end{bmatrix}$	$\begin{bmatrix} \mathbf{1} & 0 \\ 0 & \mathbf{1} \end{bmatrix}$	-0.4973	1.0e-03 * -0.6533	0.6471	1.0e-03 * 0.3653
2	$\begin{bmatrix} \mathbf{10} & 0 & 0 & 0 & 0 & 0 \\ 0 & \mathbf{0} & 0 & 0 & 0 & 0 \\ 0 & 0 & \mathbf{10} & 0 & 0 & 0 \\ 0 & 0 & 0 & \mathbf{1} & 0 & 0 \\ 0 & 0 & 0 & 0 & \mathbf{1} & 0 \\ 0 & 0 & 0 & 0 & 0 & \mathbf{10} \end{bmatrix}$	$\begin{bmatrix} \mathbf{1} & 0 \\ 0 & \mathbf{1} \end{bmatrix}$	-0.4951	1.0e-03 * 0.0026	0.6449	1.0e-03 * -0.0013
3	$\begin{bmatrix} \mathbf{0} & 0 & 0 & 0 & 0 & 0 \\ 0 & \mathbf{0} & 0 & 0 & 0 & 0 \\ 0 & 0 & \mathbf{0} & 0 & 0 & 0 \\ 0 & 0 & 0 & \mathbf{25} & 0 & 0 \\ 0 & 0 & 0 & 0 & \mathbf{25} & 0 \\ 0 & 0 & 0 & 0 & 0 & \mathbf{100} \end{bmatrix}$	$\begin{bmatrix} \mathbf{1} & 0 \\ 0 & \mathbf{10} \end{bmatrix}$	-0.2963	1.0e-03 * 0.0032	0.4463	1.0e-03 * -0.0045
4	$\begin{bmatrix} \mathbf{0} & 0 & 0 & 0 & 0 & 0 \\ 0 & \mathbf{0} & 0 & 0 & 0 & 0 \\ 0 & 0 & \mathbf{0} & 0 & 0 & 0 \\ 0 & 0 & 0 & \mathbf{500} & 0 & 0 \\ 0 & 0 & 0 & 0 & \mathbf{500} & 0 \\ 0 & 0 & 0 & 0 & 0 & \mathbf{1000} \end{bmatrix}$	$\begin{bmatrix} \mathbf{10} & 0 \\ 0 & \mathbf{500} \end{bmatrix}$	-0.2346	1.0e-03 * 0.0310	0.3846	1.0e-03 * 0.5519
5	$\begin{bmatrix} \mathbf{0} & 0 & 0 & 0 & 0 & 0 \\ 0 & \mathbf{0} & 0 & 0 & 0 & 0 \\ 0 & 0 & \mathbf{0} & 0 & 0 & 0 \\ 0 & 0 & 0 & \mathbf{500} & 0 & 0 \\ 0 & 0 & 0 & 0 & \mathbf{500} & 0 \\ 0 & 0 & 0 & 0 & 0 & \mathbf{1500} \end{bmatrix}$	$\begin{bmatrix} \mathbf{5} & 0 \\ 0 & \mathbf{500} \end{bmatrix}$	-0.1718	1.0e-03 * -0.7194	0.3218	1.0e-03 * 0.3206

The scenario used to compare the effects of these different weighting matrices is the tracking of a target that is maintaining course at a heading of zero degrees, or in the positive x direction. The initial vehicle heading error and position error was kept to a minimum before simulation was begun in order to accurately capture the effects of each

set of weighting matrices on the entire system. The speed of the tracking vehicle in each case is initially much less than that of the target vehicle, so there is a catch up phase that is required in each simulation. This was done to accurately assess how the limits on the control inputs were affecting the overall response of the system.

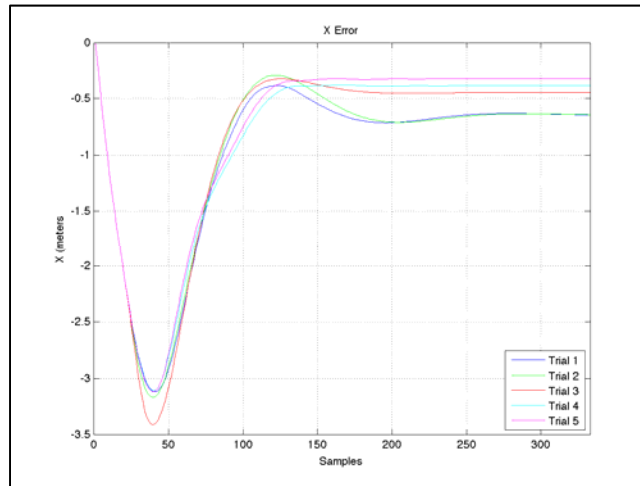


Figure 4.3 Comparison of position and error on the x axis

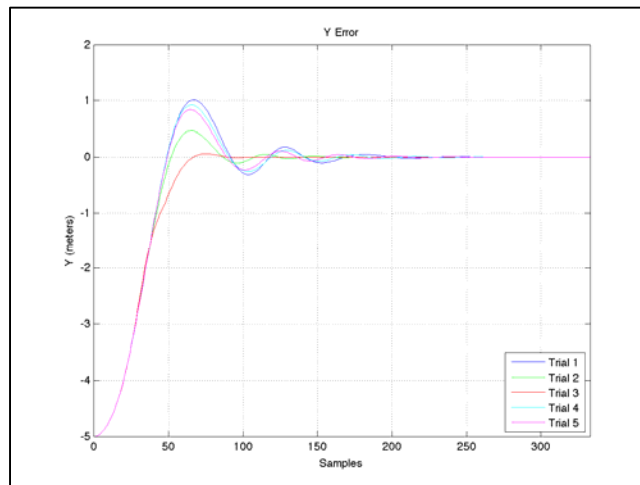


Figure 4.4 Comparison of position and error on the y axis

The first comparison in terms of controller performance due to these different weighting matrix sets will be the ability to remain on the computed reference path. Since the tracking path of the target vehicle and thus the reference path is a zero degree angle, it is reasonable to say that any error in the x direction is equivalent to the longitudinal error between the tracking vehicle and the reference path. Similarly, any error in the y direction is equivalent to the lateral error between the tracking vehicle and reference path. This is in fact the case as we can see in Figure 4.3 and Figure 4.4. We can see from these tracking errors that the weighting matrices which have the first three states weighted with zero are able to reduce the earth-fixed position error more rapidly. It will be more clear why this happens once the controls for each of these cases is examined more closely.

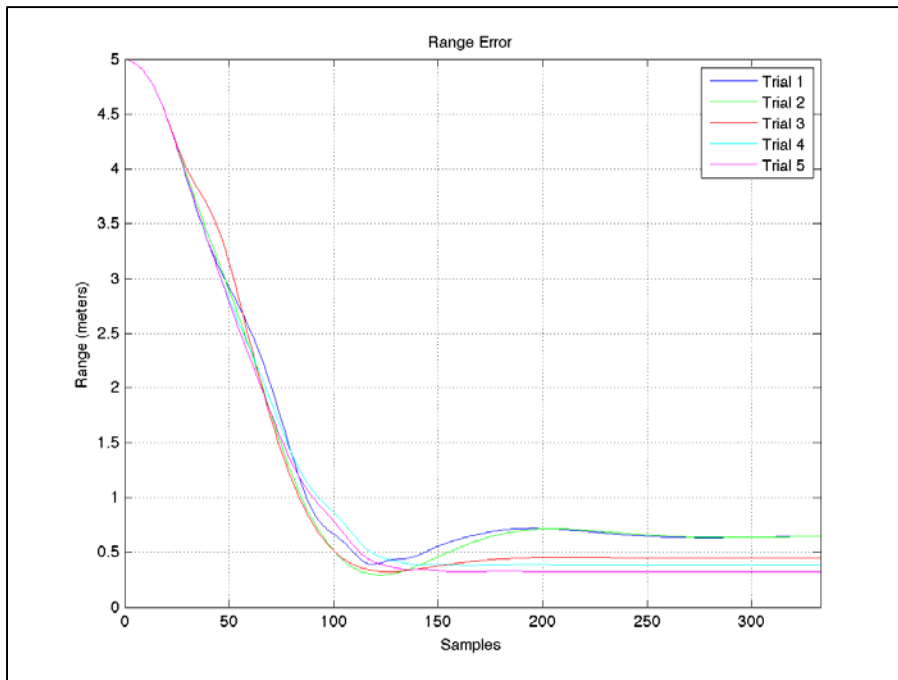


Figure 4.5 Deviation from Target Tracking Distance

Figure 4.5 shows the position of the tracking AUV in relation to the target in terms of the LOS distance for each weighting matrices trial. We can see from the range deviation plot that the vehicle is moving much slower than the target when it is first detected and tracking is initialized. There is a time period when the tracking vehicle is required to catch up to the desired tracking distance of the target. However, as expected the last three sets of weighting matrices are able to provide the system with maximum input thrust initially to begin tracking. The set distance to keep from the target as defined in these simulations is 15 meters. We can see that the set of weighting matrices used in Trial 5 have the lowest LOS error at the steady-state value. It can also be seen here that the final steady state error in the range deviation is not zero. This is most likely the cause of a design trade off that was induced by weighting the heading angle and rudder deflection more heavily than the other states.

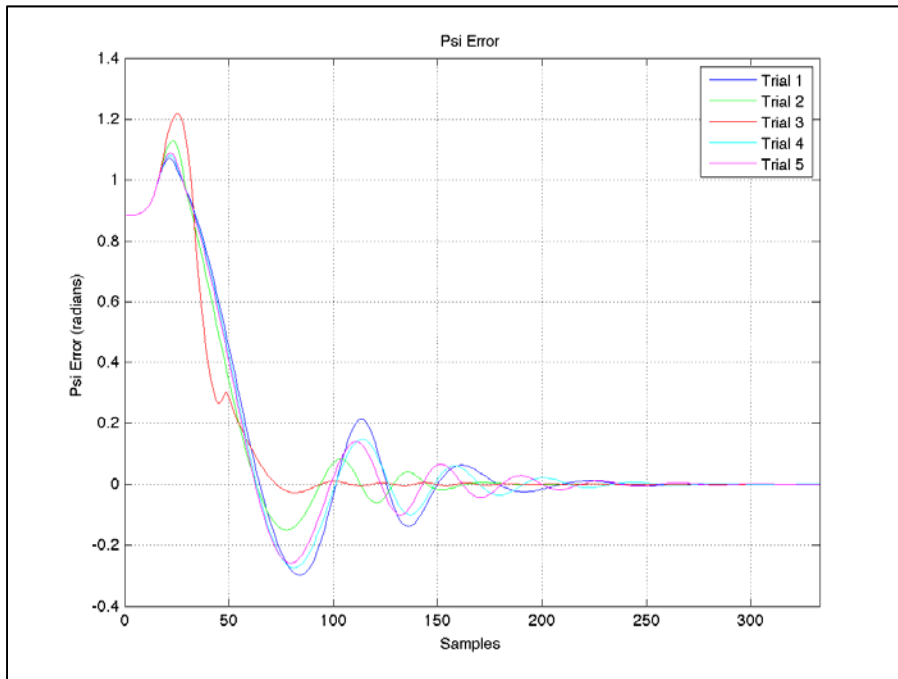


Figure 4.6 Comparison of Heading Error

The error in heading between the incremental path angle and the vehicle heading angle is shown in Figure 4.6. It is clear in this figure that all of the trial simulations result in a control system that allows the tracking AUV to maintain the same heading and path as the target.

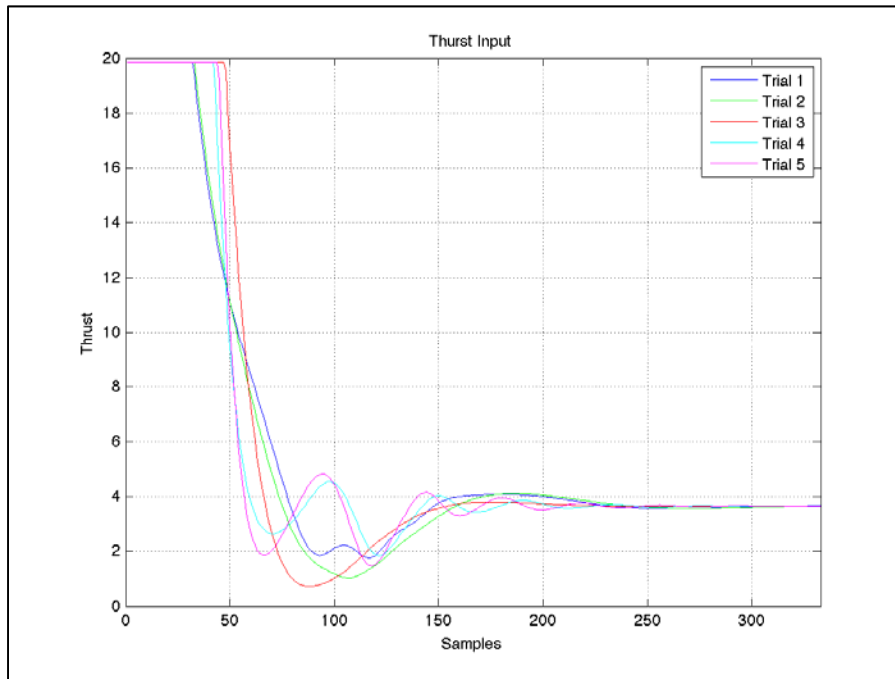


Figure 4.7 Comparison of Required Thrust Input

The final metrics that we can look at for performance comparison are the control inputs to the system. The thrust input histories for each of the trials is show in Figure 4.7 and can be used to help verify some of the previous observations in the state trajectories. Since the LQ tracker control for this design has a parameter that requires the desired translational velocity be equal to that of the target, as a reference input, the steady state thrust input for all five trials is equivalent. The translational velocity of the target can be determined by simple computation of subsequent positions and time between samples.

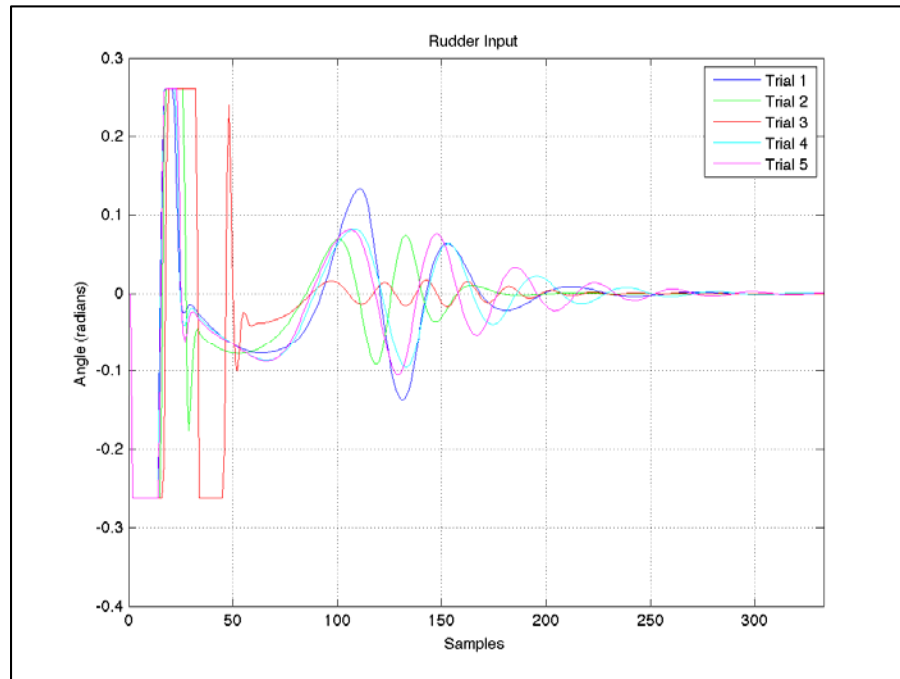


Figure 4.8 Comparison of Required Rudder Input

Figure 4.8 shows the rudder input histories for each of the trials taken in this section. The final steady-state rudder input for each of these trials goes to zero, which is expected because the target is on a straight-line course with a fixed heading angle. So, once the tracking AUV is on the path there is only minimal rudder input required to maintain this course. It is very interesting to see the different effects of the weights on the rudder control in this comparison. We can clearly see that the weighting matrices in Trial 3 result in a rudder control that more typically resembles a bang-bang solution for the first period of the simulation. Trial 1 has the smoothest rudder input in terms of overshoot, but this is the set of weights that causes the most error in tracking distance and absolute position. The performance weights that provided the best overall tracking behaviors are the ones that have relatively high values and the longest settling time. It is

evident in Figure 4.8 that once the first trial simulations have settled to a near zero rudder deflection angle, there is still significant movement of the rudder of the final two trial simulations. However, this is not dramatic enough to induce an uncontrolled response from the vehicle; these additional oscillations of the rudder are approximately ten percent of the maximum rudder deflection, and were not seen to have any erratic effects on the behavior of the system.

As expected, the pair of weighting matrices that provide the most weight on the final three systems states and have the precise recommended ratio for the diagonalized coefficients for the R weighting matrix provide the best performance.

#### **4.8. Selected Control Summary**

It was evident from the previous section that there was still a minor error in the steady state tracking range of the LQ controller proposed. Therefore, to help reduce but not completely eliminate this effect, the introduction of an additional control to thrust was applied.

From the comparison of the five trials for different weighting matrices summarized in this chapter, it was determined to use the final set of weighting matrices for further simulations. Therefore, the following matrices will be used in the performance criteria for each of the vehicle controllers used in the remainder of this thesis:

$$Q = \begin{bmatrix} \mathbf{0} & 0 & 0 & 0 & 0 & 0 \\ 0 & \mathbf{0} & 0 & 0 & 0 & 0 \\ 0 & 0 & \mathbf{0} & 0 & 0 & 0 \\ 0 & 0 & 0 & \mathbf{500} & 0 & 0 \\ 0 & 0 & 0 & 0 & \mathbf{500} & 0 \\ 0 & 0 & 0 & 0 & 0 & \mathbf{1500} \end{bmatrix}, \quad R = \begin{bmatrix} \mathbf{5} & 0 \\ 0 & \mathbf{500} \end{bmatrix}$$

The steady-state LQR feedback gain that will be used for further simulation of this thesis work is:

$$K = \begin{bmatrix} 24.7417 & 0 & 0 & 6.3298 & 7.7417 & 0 \\ 0 & 9.6012 & 0 & 0 & 0 & -3.0132 \end{bmatrix}$$

#### 4.9. Numerical Integration Techniques

An important part of this problem is the technique chosen for simulation, as this requires the iterative solution of ordinary differential equations. The most basic approach to this is Euler's Method of approximation:

$$x(t + 1) = x(t) + f(t, x(t)) * \Delta t \quad (7.32)$$

However, this approximation is not precise enough to allow for simulation of this nonlinear system. Because of this, nonlinearity the estimation error grows too quickly without bound. A more reasonable and commonly used technique is the Runge-Kutta 4<sup>th</sup> Order approximation as described in equation 4.33.

$$x(t + 1) = x(t) + \frac{(k1 + 2k2 + 2k3 + k4)}{6} \quad (7.33)$$

where:

$$k1 = f(t, x(t)),$$

$$k_2 = f\left(t + \frac{h}{2}, x(t) + \frac{h}{2}k_1\right),$$

$$k_3 = f\left(t + \frac{h}{2}, x(t) + \frac{h}{2}k_2\right),$$

$$k_4 = f(t + h, x(t) + hk_3)$$

## CHAPTER 5: Cooperative Control

So far this thesis has dealt with the development of the individual vehicle control in tracking a reference input command in order to follow a computed path based on a target's motion. However, the desired result is to have a group of AUVs performing this duty simultaneously in a cooperative manner. This will be the final step in the development of this thesis work: determine a cooperative control algorithm to coordinate multiple vehicles to perform this task as a group. There are many reasons for wanting to track a target in a group rather than just search for targets individually. Some of these reasons could be:

- i. Redundancy in case a tracking vehicle malfunctions
- ii. Increased reconnaissance computational power to detect, classify a target, and/or relay information
- iii. Grouping of vehicles remains in tact given the scenario that tracking behavior is aborted and a further search strategy

All of these reasons for tracking a target with a group of vehicles in formation are reasonable in practice, but others can be included to this list depending on the specific mission objective. In an ever-evolving world of military superiority, as well as research for further global understanding, there is an almost limitless bound of mission objectives

that can be introduced. Therefore, it is not the intent of this thesis to focus on the reasons for formation tracking, but rather the steps required to perform such actions.

For this AUV group formation, each vehicle is given a unique number in the group to determine proper alignment with the other vehicles in formation. This is key for a successful coordinated formation control algorithm that allows for the loss of a vehicle, even the “center” vehicle, to not negatively affect the formation of the remaining vehicles. This also opens up the ability for a formation that can be changed dynamically for each task of a complicated mission. If one formation is required during search, another during tracking, and another during a final stage of tracking, this approach has been developed so that a dynamic change in formation is possible.

If each vehicle’s controller understands what a specific vehicle index means, then the robustness of the group routine can be expanded. This expansion could be to allow for complex formations or the ability to separate the group when a subset of vehicles is needed to perform another task. This could be especially useful in the case where multiple target tracking is required by a large group of AUVs in a littoral environment.

Rather than deal with all the possible combinations of search and tracking formation strategies, the problem will be reduced to a single formation for searching and a single formation for tracking. We will be using a formation size of three vehicles for this research, but this approach can easily be adapted for an expanding number of group vehicles.

An assumption made up to this point is that each of the vehicles in the formation has identical kinematic models, and therefore, has the same maneuvering capabilities.

This will be an important simplification in the simulation of these coordinating vehicles because the same LQ tracking controller will be used for each vehicle. It is the outer loop control for each of these vehicles that will be manipulated in this cooperative control strategy.

### **5.1. Search formation**

While in a searching mode, the vehicles will attempt to maintain a triangular formation. This will provide for an increased range of detection as each of the individual vehicle's acoustic detection processing can cover a broader range with less overlap. All of the vehicles will maintain a specified heading angle, while the outer vehicles will maintain some predetermined lateral and longitudinal distance from the formation lead vehicle. This formation scheme is shown graphically in Figure 5.1 with the range of detection for each vehicle represented by a circular distance from the center of each vehicle.

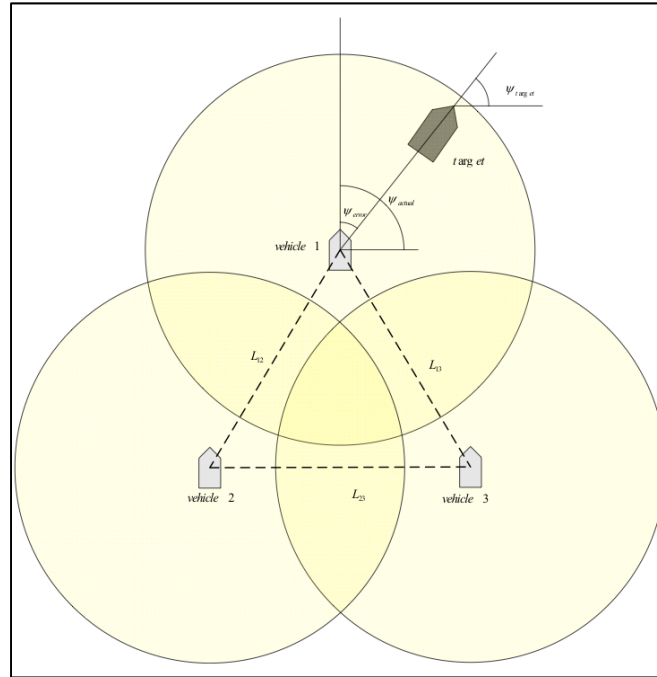


Figure 5.1 Formation for Search Formation

## 5.2. Tracking formation

Once a target vehicle has been detected within the range of any one of the AUVs in the search formation, a tracking mode will be initialized. The first task undertaken by each tracking AUV is to compute the initial reference input that will drive the initial response to correct for the error between current vehicle position and heading with respect to the desired position on the reference path. This will then allow each of the vehicles to maneuver independently to the generated reference trajectory to continue tracking the target.

Figure 5.2 shows the formation for the cooperating group in the tracking routine of this thesis. Unlike the formation of the search routine, this tracking formation will provide that each of the vehicles maintain some fixed, predetermined distance between

them. While this may not be the ideal condition for certain mission objectives, it does allow for good real time comparison of how each of the vehicles is responding to the tracking control algorithm that will be explored further in Chapter 6.

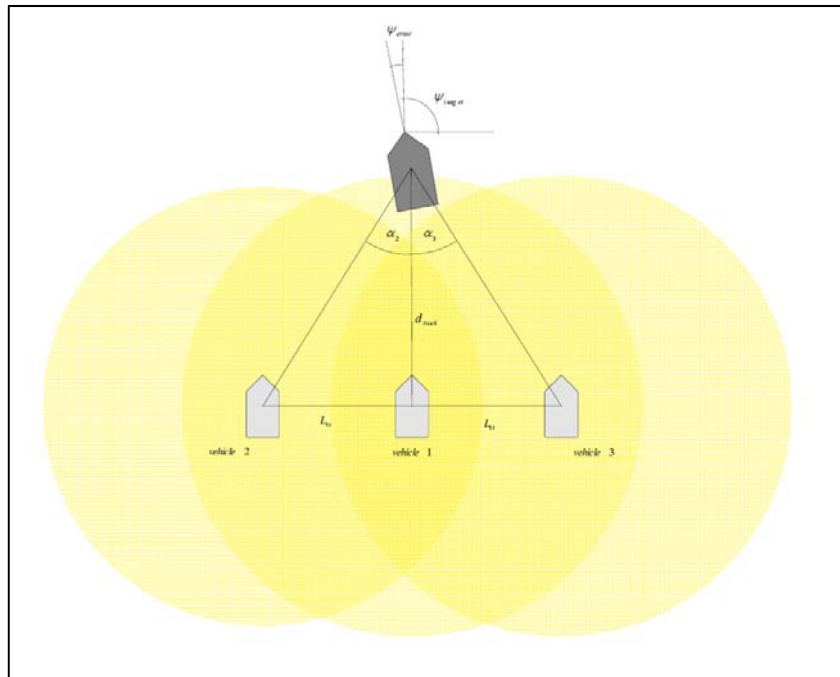


Figure 5.2 Proposed Formation for Target Tracking

Another representation of the components that are required for each of the vehicles in the formation is shown using a flow diagram in Figure 5.3. We can see from this figure that the lead vehicle requires all of the information about the target in order to compute its reference path. This lead, or center, vehicle does not require any information about the other two vehicles in the formation. The goal of this vehicle is to do the best job in tracking the target precisely. However, the outer two vehicles need information from both the target and the lead vehicle as depicted in Figure 5.3.

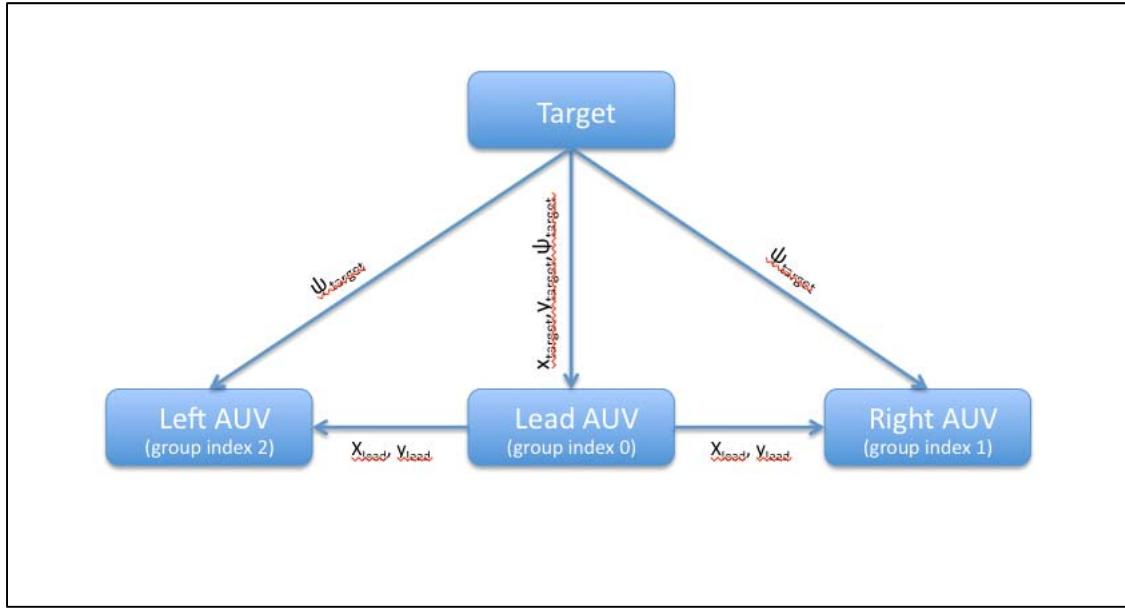


Figure 5.3 Information Flow Required for Reference Computation

The vital equations for the lead tracking AUV to compute a desired reference path are given by:

$$\dot{x}_{lead} = x_{target} - L \cos \left( \text{atan} \left( \frac{y_{target} - y_{lead}}{x_{target} - x_{lead}} \right) \right) \quad (8.1)$$

$$\dot{y}_{lead} = y_{target} - L \sin \left( \text{atan} \left( \frac{y_{target} - y_{lead}}{x_{target} - x_{lead}} \right) \right) \quad (8.2)$$

$$\dot{\psi}_{lead} = \text{atan} \left( \frac{y_{target} - y_{lead}}{x_{target} - x_{lead}} \right) \quad (8.3)$$

Each of the vehicles to either side of the lead vehicle will try and compute a similar reference trajectory, with a couple of slight modifications. The equations required for each of these vehicles is characterized by:

$$\dot{x}_{ix} = x_{lead} - (-1)^{ix} W \sin(\psi_{target} - \psi_{ix}) \quad (8.4)$$

$$\dot{y}_{ix} = y_{lead} - (-1)^{ix} W \cos(\psi_{target} - \psi_{ix}) \quad (8.5)$$

$$\dot{\psi}_{ix} = \psi_{target} - atan\left(\frac{y_{lead} - y_{ix}}{x_{lead} - x_{ix}}\right) \quad (8.6)$$

where  $ix$  is the given vehicle index in the formation and  $W$  is the desired distance between the tracking vehicles.

It will also be desired that each of the vehicles include in their reference command the desired values of the actual vehicle states. That is, the following relationships are maintained by the controller in each of the tracking vehicles:

$$u_{ix} = speed_{target} \quad (8.7)$$

$$v_{ix} = 0 \quad (8.8)$$

$$r_{ix} = 0 \quad (8.9)$$

where  $ix$  is the given vehicle index in the formation.

Equations 3.1 to 3.9 are used by each of the vehicles in formation to generate a desired reference trajectory. This path is computed online due to the fact that the target has the ability to change course at any given time within the simulation. It is assumed for a marine craft that the heading angle must be smooth, as sudden changes in heading angle are not possible by the target vehicle.

The ability of the algorithms that will be used to both compute the desired reference trajectory, as well as the initial transition from search pattern to tracking formation will be tested in detail in chapter 6. This section has provided background and

visual information that is necessary to understand how each of the vehicles in the cooperating group formation is expected to behave.

## **CHAPTER 6: Simulation and Results**

### **6.1. Introduction**

This chapter will help conclude the control algorithm that has been developed for this thesis work. Three scenarios will be presented separately to display the ability of the target tracking algorithm to perform based on different initial conditions, as well as different target motion characteristics. The abilities of this control technique will be evaluated for each one of these scenarios based on overall performance. The control inputs required will be studied to try to examine the effectiveness of the group at tracking a target, as well as the robustness of the controller design.

### **6.2. Scenario 1**

The first scenario that will be presented is the most basic in its performance demands from the tracking group. This scenario is started when the AUV formation has detected a target in front of the lead vehicle, but is calculated to have a heading different from that of the group. The heading of the target is computed to be 60-degrees while the AUV formation is maintaining a search pattern with a 90-degree heading. Once the target vehicle is detected, each AUV in the group is required to compute a desired reference path for tracking. This reference path will then allow each of the vehicles in the formation to perform the desired tracking pattern.

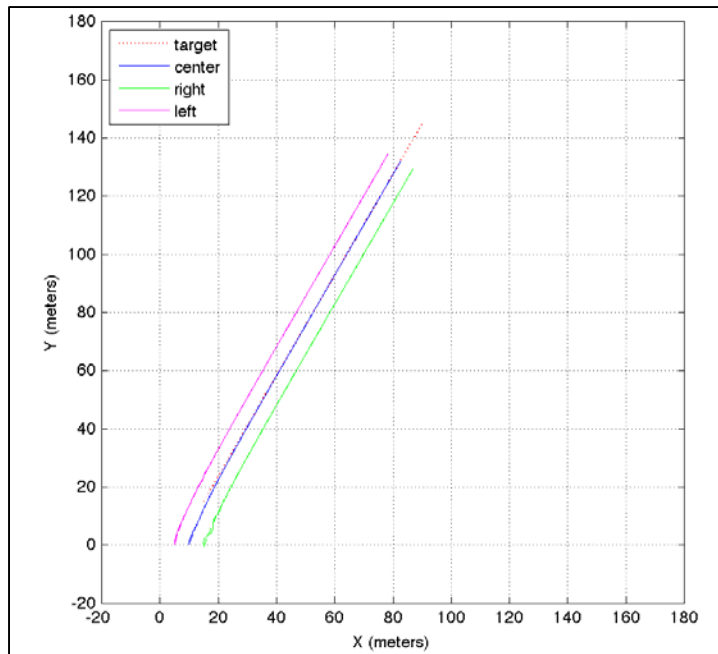


Figure 6.1 XY Plot for Tracking a Target with Constant Heading

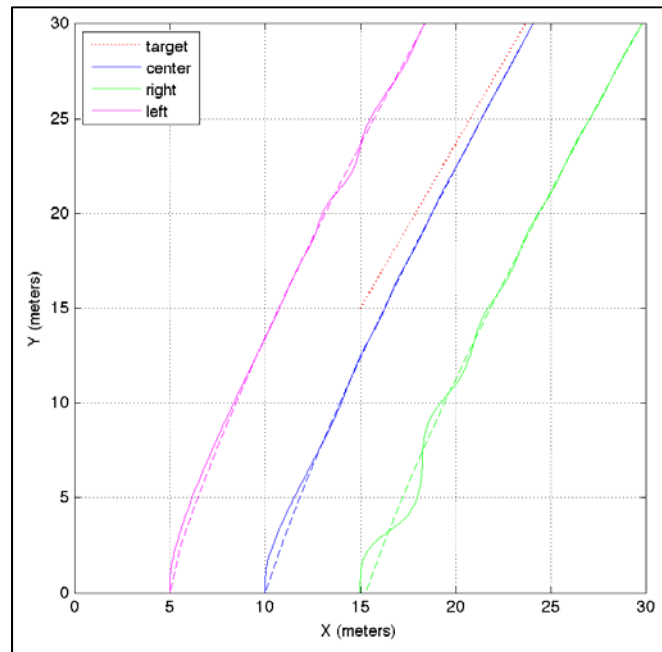


Figure 6.2 Zoomed in on Beginning of Tracking for Target with Constant Heading

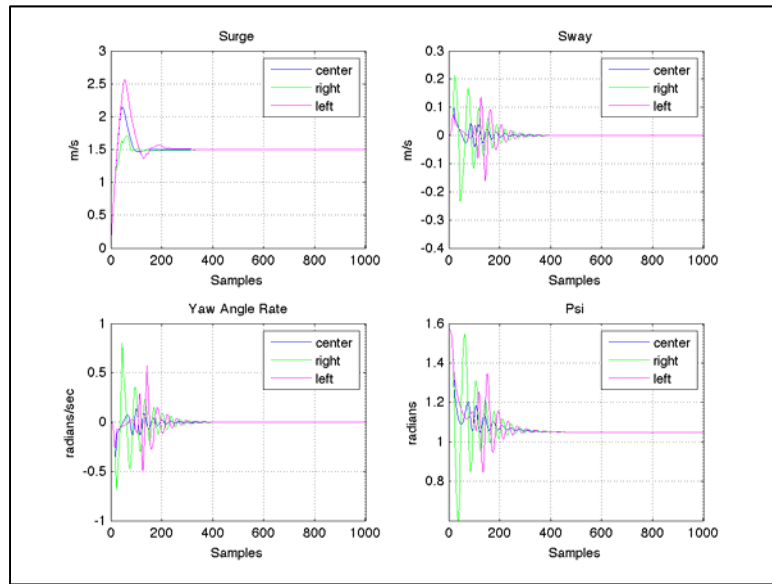


Figure 6.3 Vehicle States for Tracking Target with Constant Heading

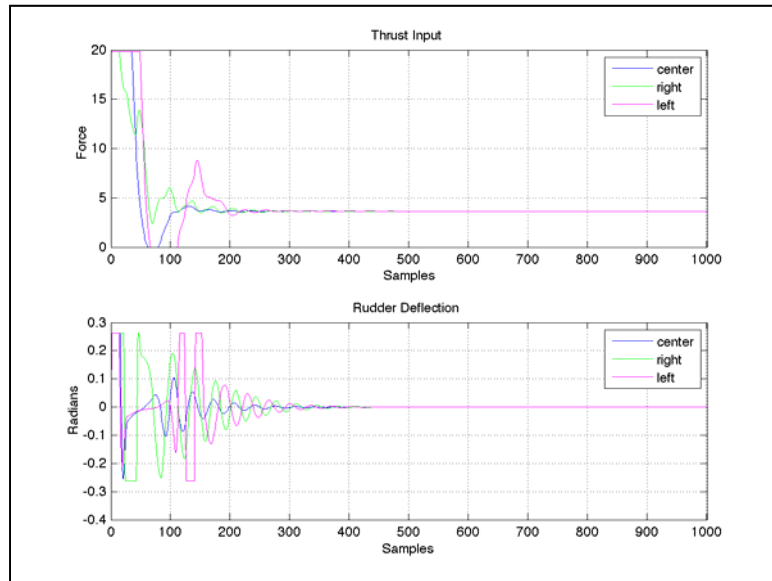


Figure 6.4 Control Inputs for Target Tracking with Constant Heading

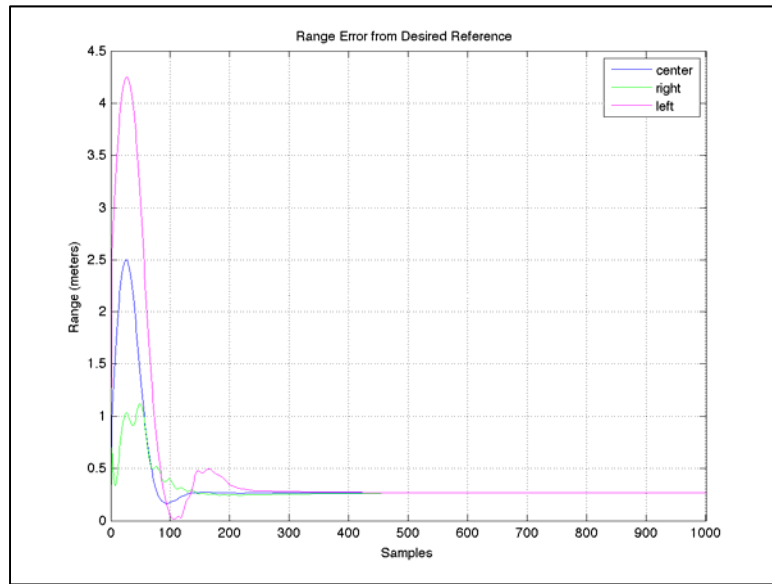


Figure 6.5 Range Error from Reference for Target with Constant Heading

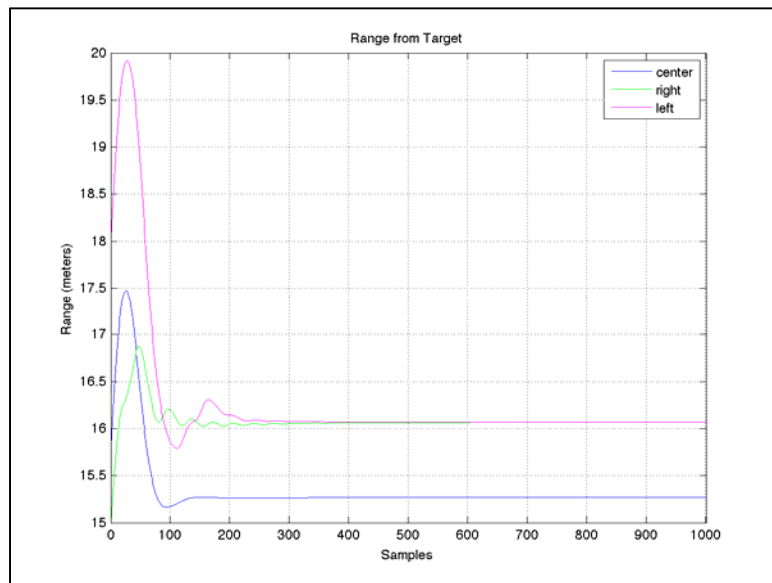


Figure 6.6 Tracking Range from Target with Constant Heading

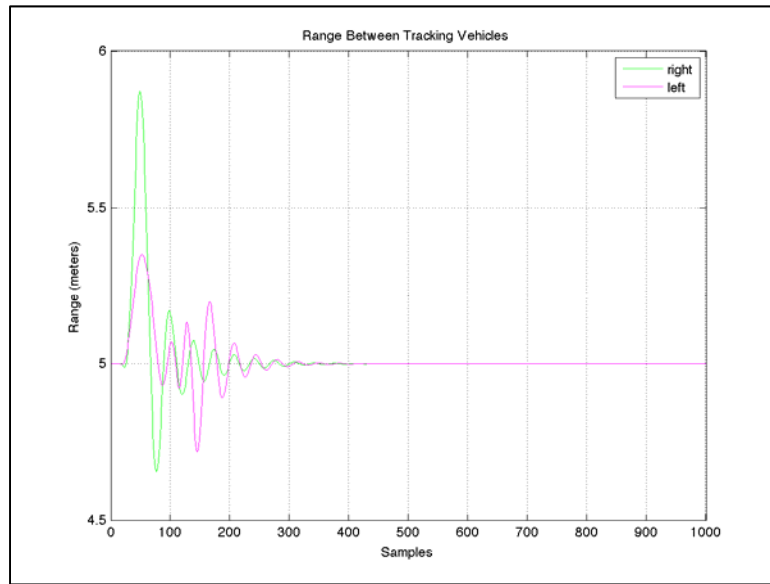


Figure 6.7 Range Between Tracking Vehicles

From this scenario, it is shown that the tracking algorithm developed is sufficient to detect and begin tracking a known target. Figure 6.1 shows that the overall group tracking of the target detected performs as desired. The transition from the search pattern to the tracking pattern is further detailed in Figure 6.2. Once the detection was made, the tracking vehicles were able to compute and precisely track their reference trajectory. In Figure 6.3 and 6.4 not only is the vehicle motion detailed, but also the control inputs that are required to get the vehicle to the path that is calculated for tracking. This shows that the initial corrections are made by each of the vehicles and then steady out to their desired final values to allow constant following where the speed of the group is equal to the speed of the target vehicle.

Figures 6.5 and 6.6 depict the range between the desired reference trajectories and the target position respectively. These histories show that there is minimal tracking error

in terms of overall range from the target. This error is most likely the result of the performance trade off from the design to place a majority weight in the vehicles' ability to maintain heading as a priority. Figure 6.7 shows that while each vehicle is transitioning to the tracking formation, that their spacing is changing but eventually stabilizes to a desired equal distance between each vehicle.

### **6.3. Scenario 2**

The second scenario that will be presented is slightly more difficult in the maneuverability that is required for each of the vehicles in the tracking group. This scenario is started when the AUV formation has detected a target that has the same direction of track and heading as the group, but offset to the side of the formation as opposed to scenario 1. Once the target is detected, the vehicle formation will have to re-align itself with the tracking pattern that is desired. This requires a sideways shift by all of the vehicles in the group.

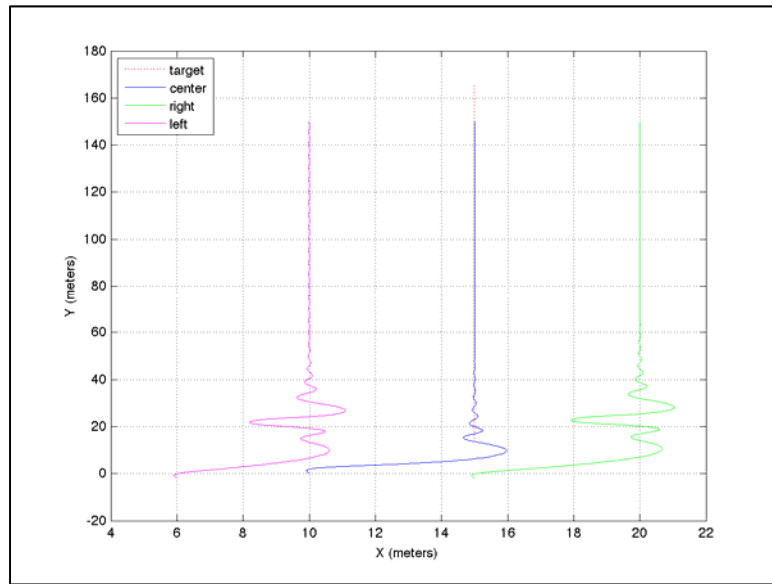


Figure 6.8 XY Plot for Target Tracking with Offset Position

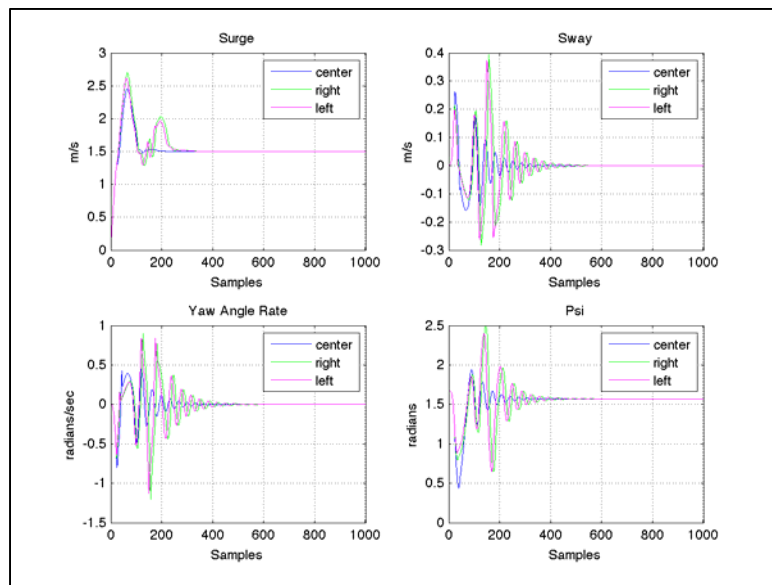


Figure 6.9 Vehicle States for Target Tracking with Offset Position

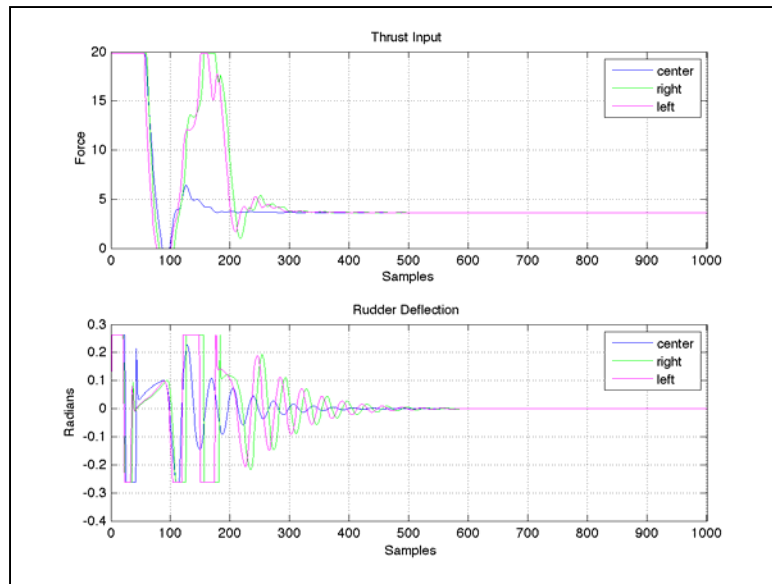


Figure 6.10 Control Inputs for Tracking Target with Offset Position

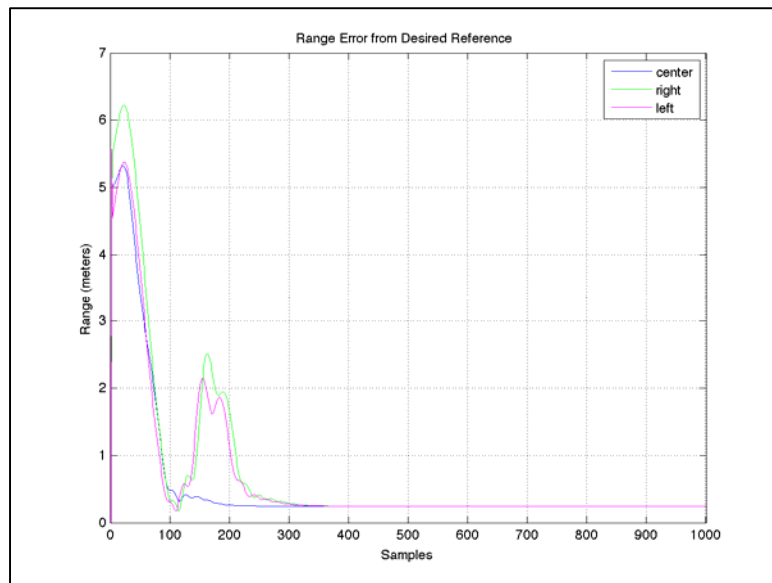


Figure 6.11 Range Error from Reference for Target with Offset Position

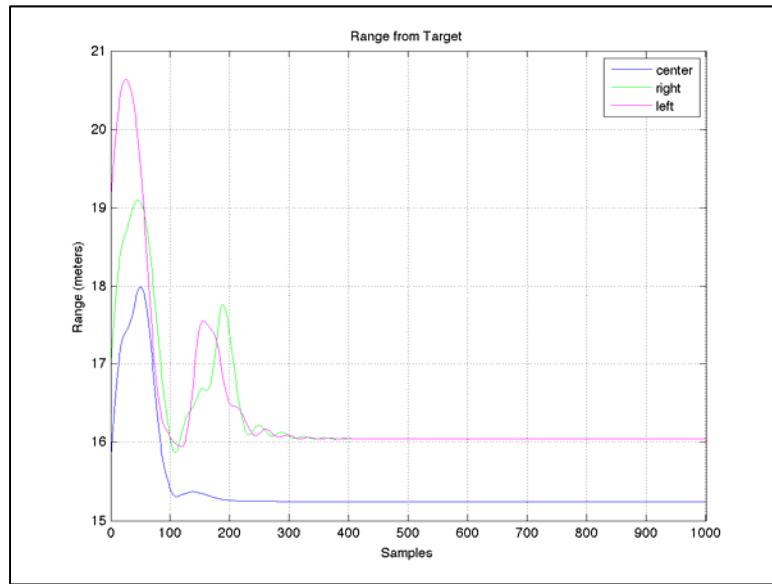


Figure 6.12 Tracking Range from Target with Offset Position

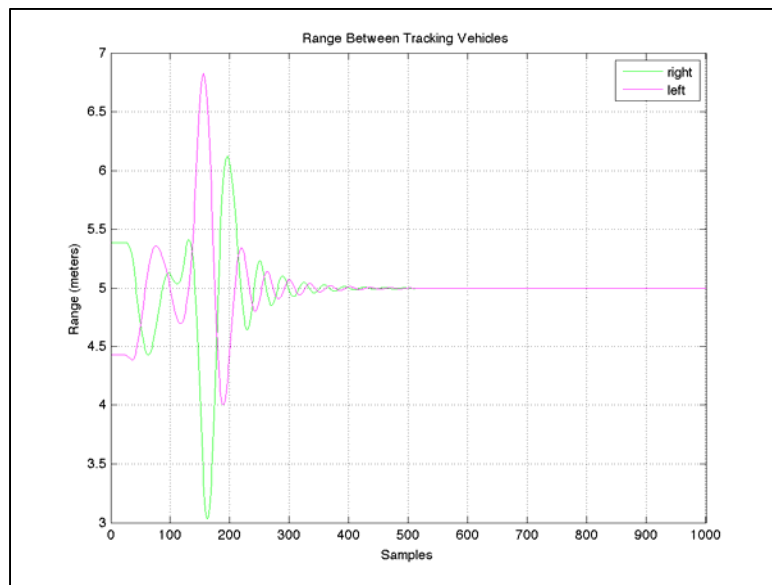


Figure 6.13 Range Between Tracking Vehicles

It is clear from this scenario that the maneuvering for this case is more significant than that from the more basic first scenario. Figure 6.8 shows that the overall correction

of this offset position between target and tracking formation results in the desired tracking behavior. The oscillations in position and the heading for each vehicle, is due to the individual vehicles in the formation trying to account for the position of the other vehicles in the group. While this may not be the ideal path for any individual vehicle, it is required to maintain formation spacing that will ultimately result in a protection from collision of the tracking AUVs. In figure 6.9 it is clear that the center vehicle is essentially the lead for this formation because this vehicles states converge to their steady state values more rapidly that the other vehicles in formation. This resulting vehicle behavior is explained by referencing figure 6.10 in that the outer two vehicles require more thrust and rudder input than the center vehicle.

Figures 6.11 and 6.12 depict the range between the desired reference trajectories and the target position respectively. These histories show that there is minimal tracking error in terms of overall range from the target. As seen in the previous scenario, the error in overall tracking range remains and is again most likely the result of a performance tradeoff. Figure 6.13 shows again that while each vehicle is transitioning to the tracking formation, their spacing is changing, but eventually stabilizes to a desired equal distance between each vehicle.

#### **6.4. Scenario 3**

The final scenario that will be presented is significantly different from the previous two. The first two scenarios dealt with tracking a target that maintained a fixed heading throughout the run. This scenario will show the performance of the cooperative

tracking algorithm developed when the target abruptly changes its heading angle. This is not entirely a feasible path to follow in that marine vehicle generally cannot change its heading suddenly. There must be some length of time in which the heading is either increasing or decreasing, that is, the target vehicle will possess some bearing rate over this time period. Bearing rate is the term used to briefly describe a vehicle's ability to change its direction over a given period of time. The tracking vehicles will be required to detect this change in heading and modify the reference path that will be followed to incorporate this new direction. As detailed in chapter 5, the reference path that is computed will contain a smooth estimate of the heading change to aid in reasonable tracking behavior.

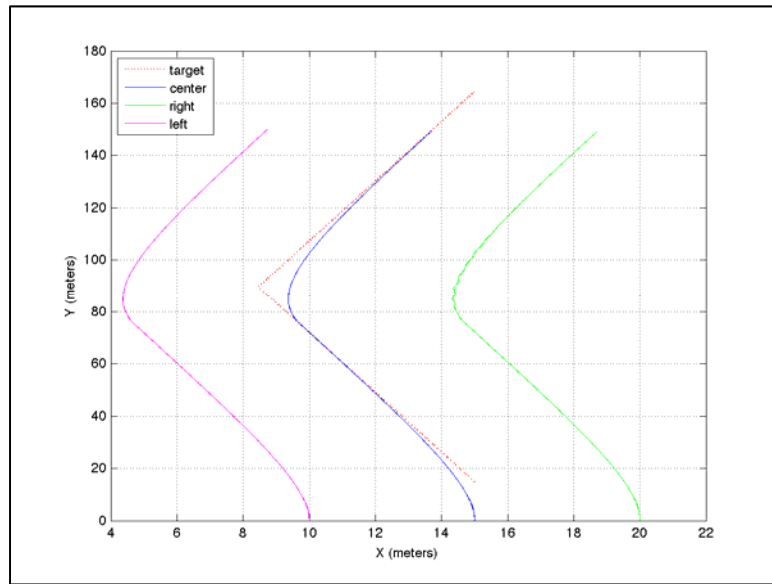


Figure 6.14 XY Plot for Tracking Target Through Heading Change

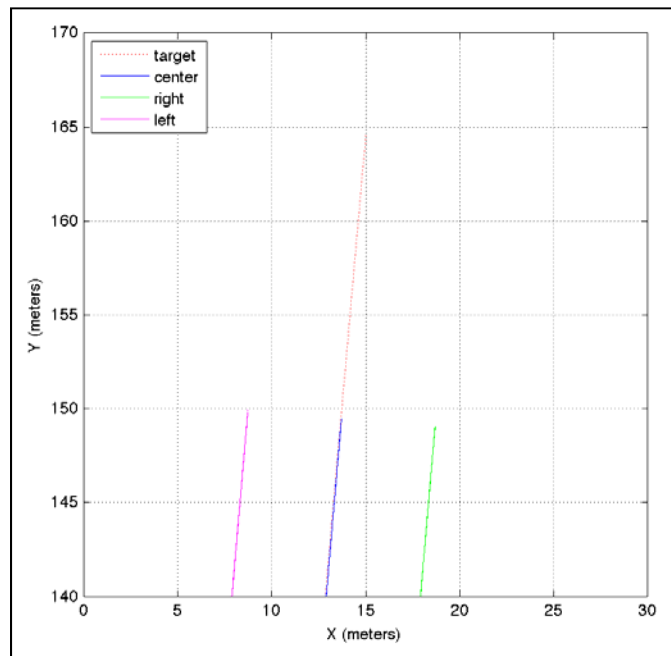


Figure 6.15 Zoomed in on End of Tracking Target Through Heading Change

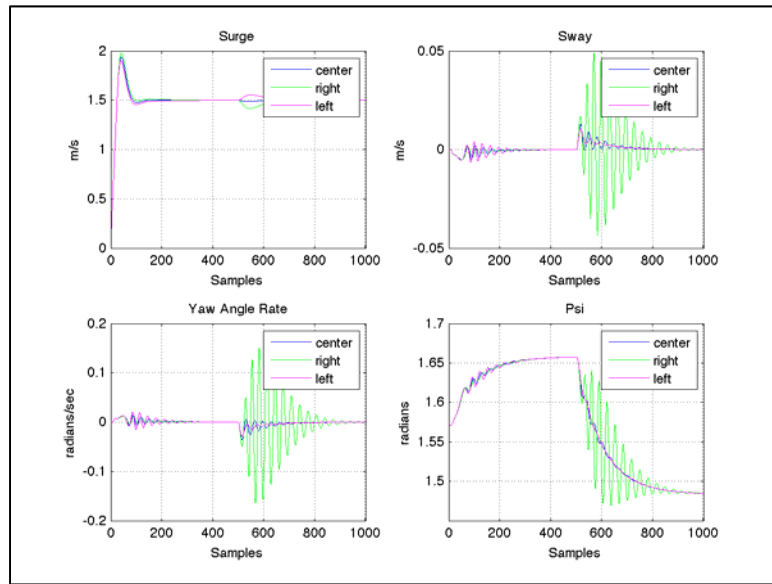


Figure 6.16 Vehicle States While Tracking Target Through Heading Change

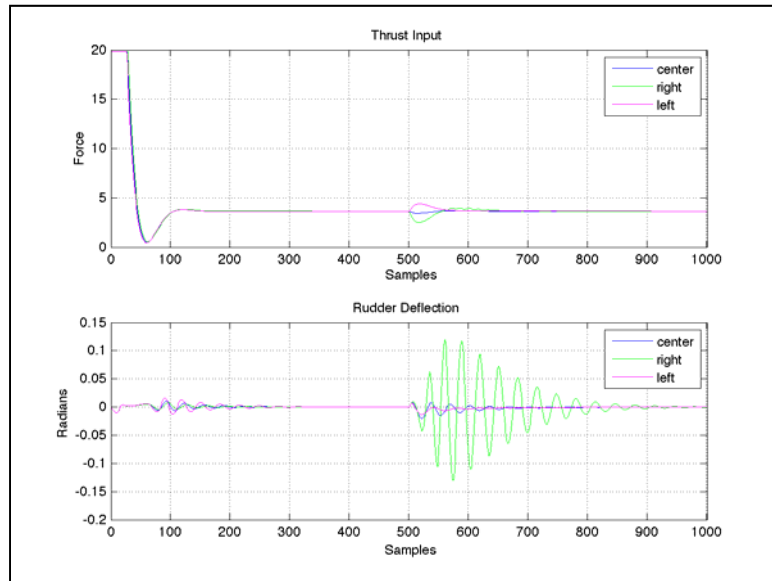


Figure 6.17 Control Inputs While Tracking Target Through Heading Change

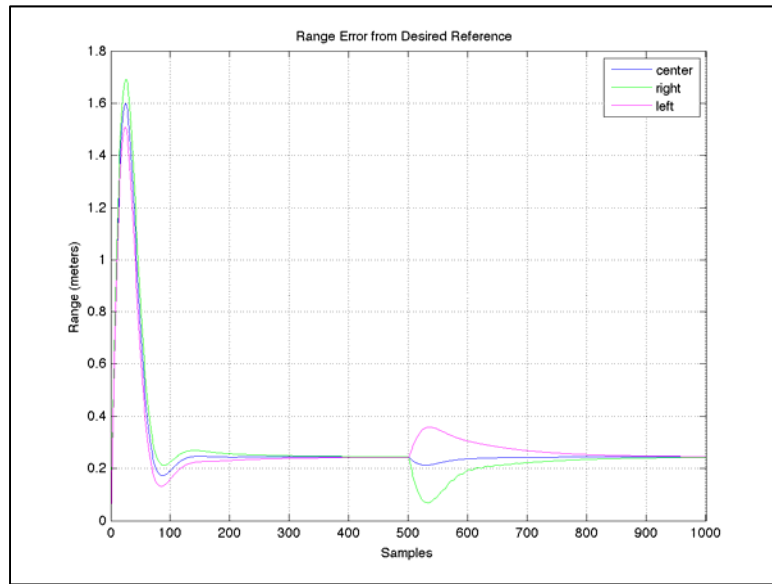


Figure 6.18 Range Error from Reference Track for Target with Heading Change

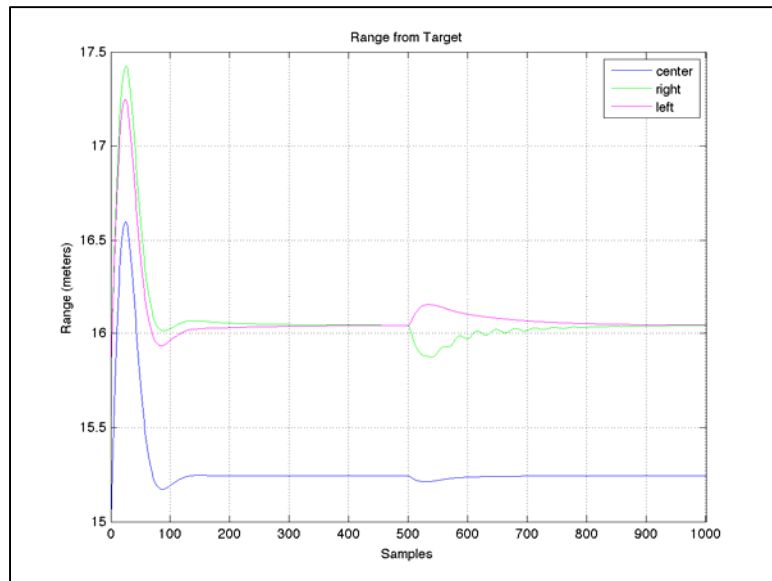


Figure 6.19 Tracking Range from Target Through Heading Change

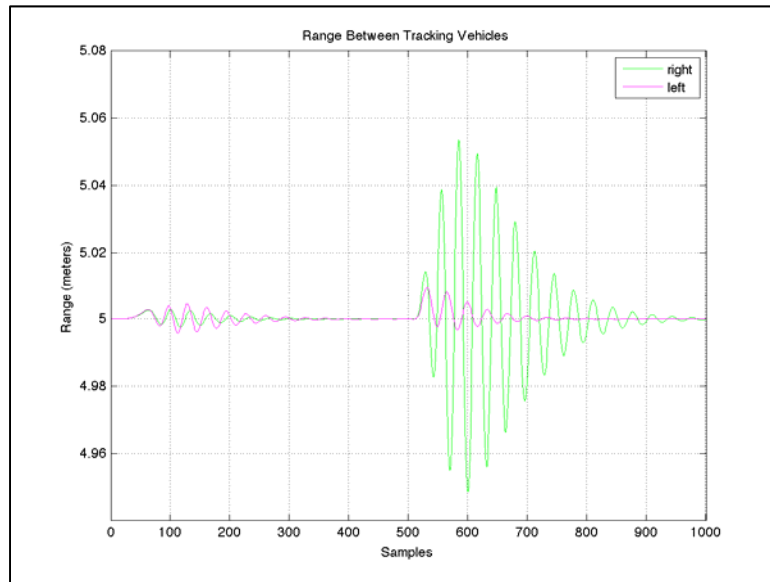


Figure 6.20 Range Between Tracking Vehicles

This final scenario depicts the most demanding tracking requirements on this cooperative control algorithm. That is vehicle formation is required to track a target through a heading change. If there is any possibility of this algorithm to fail and become unstable, it is during the tracking of a target that makes an abrupt shift in heading angle. Figure 6.14 visually concludes that the tracking formation is able to smooth the transition in heading effectively, and efficiently maintain a tracking behavior. Figure 6.17 are the control inputs to each of the vehicles in formation; the first thing that is apparent is the input rudder control on one of the vehicles during the heading transition. However, the vehicle controller is able to restrict this control action from becoming unstable and to eventually maintain a desired input. This behavior on control input is manifested in the vehicle states in Figure 6.16 that show one of the vehicles with slightly different values

that the other two AUVs in the group. While these effects may appear visually significant due to the scale of the graphs presented, they are in fact minor.

Figure 6.20 shows that while each vehicle is transitioning to the tracking formation their spacing is changing, but eventually stabilizes to a desired equal distance between each vehicle. This figure also shows that during the heading transition there is some deviation in the desired vehicle spacing, but again is corrected and results in the final desired inter-vehicle spacing. Figures 6.18 and 6.19 depict the range between the desired reference trajectories and the target position respectively, as was the case in the previous two scenarios, there is some minor steady state error.

## **CHAPTER 7: Conclusion**

### **7.1. Thesis Summary**

The dynamics of the REMUS AUV were presented in Chapter 2, where a set of equations of motion and necessary coordinate frames were also introduced. Chapter 3 developed the required technique for a vehicle to detect a target position, and generate a path to follow based on desired tracking parameters. The vehicle control algorithm was developed and studied in Chapter 4 by linearizing the known system for the AUV and then applying a LQ tracker solution. Chapter 5 introduced the fundamentals of how a group of vehicles is able to cooperate in formation to track a target. A detailed set of control scenarios was investigated and analyzed in Chapter 6 in order to prove the tracking algorithm developed in this thesis satisfied the required design specifications that were set forth in the problem definition. It was shown through these different tests that the algorithm developed in this research is effective in detecting and tracking a target while maintaining some predefined formation for the group of underwater vehicles.

### **7.2. Research Conclusions**

The work performed in this thesis research has the sufficient detail that is required to conclude that the steering model of the chosen AUV can in fact be used in conjunction with an LQ tracking control algorithm to track a reference path. This same vehicle has

been combined with other vehicles of similar dynamics in order to determine a reference path and track a detectable target as a group. The work developed was tested to show that this group formation control could indeed track a target that is moving away from the group upon initial detection. It can also track a target through a heading change should this be required. This is an important result that could have many possible uses in both military and commercial applications.

### **7.3. Proposed Future Research**

The field of cooperative control for groups of vehicles, especially underwater vehicles, is still an evolving field of research. Further research for this specific thesis approach has many different possible variations. One immediate question that can be investigated is how this control algorithm can perform in a more harsh environment that includes current, limited communication, and sparse target detection points. Detailing larger groups with a more advanced tracking formation would also be relevant research to be done. Furthermore, additional control techniques could be investigated in order to minimize some of the minor tracking errors that were found in this thesis due to design parameters. There are many other theoretical control algorithms for controlling nonlinear systems that could also be investigated. While there is still a great deal of work that could be done to advance this topic and the problem that was set forth in this thesis, this research was a vital starting point of research and provides a platform for future work.

## APPENDIX A: MATLAB Code

This appendix contains a selection of required MATLAB script files used to simulate the vehicle control proposed in this thesis.

### A.1 Vehicle Dynamics: `auvDynamics.m`

```
%-----  
% GENERAL VEHICLE PARAMETES  
%-----  
  
% Myring Paramters for STD REMUS  
  
a          = 1.91e-01;    % Nose Length          (m)  
a_offset   = 1.65e-02;    % Nose Offset         (m)  
b          = 6.54e-01;    % Midbody Length      (m)  
c          = 5.41e-01;    % Tail Length         (m)  
c_offset   = 3.68e-02;    % Tail Offset        (m)  
n          = 2.00;        % Exponential Coefficient (n/a)  
theta_tail = 4.36e-01;    % Included Tail Angle (rad)  
d          = 1.91e-01;    % Max Hull Diameter   (m)  
L_f        = 8.28e-01;    % Vehicle Forward Length (m)  
L          = 1.33;        % Vehicle Total Length (m)  
  
% REMUS Fin Parameters  
  
S_fin      = 6.65e-03;    % Platform Area          (m^2)  
b_fin      = 8.57e-02;    % Span                   (m)  
x_finpost  = -6.38e-01;   % Moment Arm wrt Vehicle Origin at CB (m)  
delta_max  = 1.36e01;    % Maximum Fin Angle      (deg)  
a_fin      = 5.14;        % Max Fin Height Aove Centerline (m)  
c_mean     = 7.47e-02;    % Mean Chord Length      (m)  
t_fin      = 6.54e-01;    % Fin Taper Ratio        (n/a)  
c_df       = 5.58e-01;    % Fin Crossflow Drag Coefficient (n/a)  
AR_e       = 2.21;        % Effective Aspect Ratio (n/a)  
a_bar      = 9.00e-01;    % Lift Slope Parameter   (n/a)  
c_lalpha   = 3.12e00;    % Fin Lift Slope        (n/a)  
  
% Center, Moments, Weights  
  
W          = 2.99e02;    % Vehicle Weight        (N)  
B          = 3.06e02;    % Vehicle Buoyancy      (N)  
x_cb       = -6.11e-01;  % Center of Buoyancy wrt Origin at Nose (m)  
y_cb       = 0.00;        % Center of Buoyancy wrt Origin at Nose (m)  
z_cb       = 0.00;        % Center of Buoyancy wrt Origin at Nose (m)  
x_cg       = 0.00;        % Center of Gravity wrt Origin at Nose (m)  
y_cg       = 0.00;        % Center of Gravity wrt Origin at Nose (m)  
z_cg       = 1.96e-02;   % Center of Gravity wrt Origin at Nose (m)
```

```

I_xx    = 1.77e-01;    % Moment of Inertia wrt Origin at CB    (kg*m^2)
I_yy    = 3.45;      % Moment of Inertia wrt Origin at CB    (kg*m^2)
I_zz    = 3.45;      % Moment of Inertia wrt Origin at CB    (kg*m^2)

```

```
% Hull Parameters for STD REMUS
```

```

rho      = 1.03e03;    % Seawater Density    (kg/m^3)
A_f      = 2.85e-02;    % Hull Frontal Area    (m^2)
A_p      = 2.26e-01;    % Hull Projected Area - xz plane    (m^2)
S_w      = 7.09e-01;    % Hull Wetted Surface Area    (m^2)
delta    = 3.15e-02;    % Estimated Hull Volume    (m^3)
B_est    = 3.17e02;    % Estimated Hull Buoyancy    (N)
x_cb_est = 5.54e-03;    % Est. Long. Center of Buoyancy    (m)

```

```
% Additional Hull Parameters
```

```

c_d      = 3.00e-01;    % REMUS Axial Drag Coefficient    (n/a)
c_dc     = 1.10;        % Cylinder Cross flow Drag Coefficient    (n/a)
c_ydBeta = 1.20;        % Hoerner Body Lift Coefficient    (n/a)
x_cp     = -3.21e-01;    % Center of Pressure    (n/a)
alpha    = 3.59e-02;    % Ellipsoid Added Mass Coefficient    (n/a)

```

```
% Hull Points and Coordinates
```

```

x_t      = -7.21e-01;    % Aft End of Tail Section    (m)
x_t1     = -2.18e-01;    % Forward End of Tail Section    (m)
x_f      = -6.85e-01;    % Aft End of Fin Section    (m)
x_f2     = -6.11e-01;    % Forward End of Fin Section    (m)
x_b      = 4.37e-01;    % Aft End of Bow Section    (m)
x_b2     = 6.10e-01;    % Forward End of Bow Section    (m)

```

```

%-----
% NON-LINEAR MANEUVERING FORCES AND MOMENTS COEFFICIENTS
%-----

```

```

% Added mass cross-terms that are 0.00 have been excluded
% Control fin cross-term coefficients have been excluded

```

```

X_uu     = -1.62;        % Cross-flow Drag    (kg/m)
X_udot   = -9.30e-01;    % Added Mass    (kg)
X_wq     = -3.55e01;    % Added Mass Cross-term    (kg/rad)
X_qq     = -1.93;        % Added Mass Cross-term    (kg*m/rad)
X_vr     = 3.55e01;    % Added Mass Cross-term    (kg/rad)
X_rr     = -1.93;        % Added Mass Cross-term    (kg*m/rad)
X_prop   = 3.86;        % Propeller Thrust    (N)
Y_vv     = -1.31e02;    % Cross-flow Drag    (kg/m)
Y_rr     = 6.32e-01;    % Cross-flow Drag    (kg*m/rad^2)
Y_uv     = -2.86e01;    % Body Lift Force and Fin Lift    (kg/m)
Y_vdot   = -3.55e01;    % Added Mass    (kg)
Y_rdot   = 1.93;        % Added Mass    (kg*m/rad)
Y_ur     = 5.22;        % Added Mass Cross Term and Fin Lift    (kg/rad)
Y_wp     = 3.55e01;    % Added Mass Cross-term    (kg/rad)
Y_pq     = 1.93;        % Added Mass Cross-term    (kg*m/rad)
Y_uudr   = 9.64;        % Fin Lift Force    (kg/(m*rad))
Z_ww     = -1.31e02;    % Cross-flow Drag    (kg/m)

```

```

Z_qq    = -6.32e-01;    % Cross-flow Drag                (kg*m/rad^2)
Z_uw    = -2.86e01;    % Body Lift Force and Fin Lift    (kg/m)
Z_wdot  = -3.55e01;    % Added Mass                      (kg)
Z_qdot  = -1.93;       % Added Mass                      (kg*m/rad)
Z_uq    = -5.22;       % Added Mass Cross-term and Fin Lift (kg/rad)
Z_vp    = -3.55e01;    % Added Mass Cross-term          (kg/rad)
Z_rp    = 1.93;        % Added Mass Cross-term          (kg/rad)
Z_uuds  = -9.64;      % Fin Lift Force                  (kg/(m*rad))

K_pp    = -1.30e-03;    % Rolling Resistance              (kg*m^2/rad^2)
K_pdot  = -1.41e-02;    % Added Mass                      (kg*m^2/rad)
K_prop  = -5.43e-01;    % Propeller Torque                (N*m)
M_ww    = 3.18;        % Cross-flow Drag                (kg)
M_qq    = -9.40;       % Cross-flow Drag                (kg*m^2/rad^2)
M_uw    = 2.40e01;     % Body and Fin Lift and Munk Moment (kg)
M_wdot  = -1.93;      % Added Mass                      (kg*m)
M_qdot  = -4.88;      % Added Mass                      (kg*m^2/rad)
M_uq    = -2.00;      % Added Mass Cross Term and Fin Lift (kg*m/rad)
M_vp    = -1.93;      % Added Mass Cross Term          (kg*m/rad)
M_rp    = 4.86;       % Added Mass Cross-term          (kg*m^2/rad^2)
M_uuds  = -6.15;     % Fin Lift Moment                (kg/rad)
N_vv    = -3.18;      % Cross-flow Drag                (kg)
N_rr    = -9.40;      % Cross-flow Drag                (kg*m^2/rad^2)
N_uv    = -2.40e01;   % Body and Fin Lift and Munk Moment (kg)
N_vdot  = 1.93;      % Added Mass                      (kg*m)
N_rdot  = -4.88;     % Added Mass                      (kg*m^2/rad)
N_ur    = -2.00;     % Added Mass Cross Term and Fin Lift (kg*m/rad)
N_wp    = -1.93;     % Added Mass Cross Term          (kg*m/rad)
N_pq    = -4.86;     % Added Mass Cross-term          (kg*m^2/rad^2)
N_uudr  = -6.15;     % Fin Lift Moment                (kg/rad)

```

```

g = 9.81;
W = 2.99e02;
m = W/g;

```

```

x_fin = x_finpost;

```

```

Y_deltar = rho*c_Lalpha*S_fin;
N_deltar = rho*c_Lalpha*S_fin*x_fin;

```

```

rudder_sat = 15;

```

```

m11=(m-X_udot);
m12=0;
m13=0;
m14=0;
m15=0;
m16=0;

```

```

m21=0;
m22=(m-Y_vdot);
m23=-Y_rdot;
m24=0;
m25=0;
m26=0;

```

```

m31=0;

```

```

m32=-N_vdot;
m33=(I_zz-N_rdot);
m34=0;
m35=0;
m36=0;

m41=0;
m42=0;
m43=0;
m44=1;
m45=0;
m46=0;

m51=0;
m52=0;
m53=0;
m54=0;
m55=1;
m56=0;

m61=0;
m62=0;
m63=0;
m64=0;
m65=0;
m66=1;

M = [ m11  m12  m13  m14  m15  m16;
      m21  m22  m23  m24  m25  m26;
      m31  m32  m33  m34  m35  m36;
      m41  m42  m43  m44  m45  m46;
      m51  m52  m53  m54  m55  m56;
      m61  m62  m63  m64  m65  m66 ];

```

## A.2 Numerical Integration: `auvProc.m`

```

function out = auvProc(X,dT,U_nonlinear)

ii = 1;
dt = dT/ii;

for k = 1:ii
    k1 = dt*f(X,U_nonlinear);
    k2 = dt*f(X+k1/2,U_nonlinear);
    k3 = dt*f(X+k2/2,U_nonlinear);
    k4 = dt*f(X+k3,U_nonlinear);
    X = X + k1/6 + k2/3 + k3/3 + k4/6;
end

out = X;

end

function dx = f(x,U_nonlinear)

auvDynamics;

```

```

% SYSTEM SIMULATION

dx = zeros(6,1);    % a column vector

dx(1) = [X_uu*x(1)*abs(x(1))+X_vr+m)*x(2)*x(3)+...
        X_rr*x(3)^2]/(m-X_udot) + U_nonlinear(1)/(m-X_udot);

dx(2) = [Y_vv*x(2)*abs(x(2))+Y_rr*x(3)*abs(x(3))+...
        (Y_ur-m)*x(1)*x(3)+Y_uv*x(1)*x(2)]/(m-Y_vdot) + ...
        (Y_deltar*x(1)^2*U_nonlinear(2))/(m-Y_vdot);

dx(3) = [N_vv*x(2)*abs(x(2))+N_rr*x(3)*abs(x(3))+...
        N_ur*x(1)*x(3)+N_uv*x(1)*x(2)]/(I_zz-N_rdot) + ...
        (N_deltar*x(1)^2*U_nonlinear(2))/(I_zz-N_rdot);

dx(4) = x(1)*cos(x(6)) - x(2)*sin(x(6));

dx(5) = x(1)*sin(x(6)) + x(2)*cos(x(6));

dx(6) = x(3);

end

```

### A.3 Feedback Control: auvControl.m

```
function [U_nonlinear,deltaU,gain] =
auvControl(Q,R,x,x_ref,ii,jj,speed,K)

    auvDynamics;

    if(ii==1)

        u      = x(1);
        v      = x(2);
        r      = x(3);
        x_pos  = x(4);
        y_pos  = x(5);
        psi    = x(6);

        a11=2*X_uu*abs(u);
        a12=(X_vr+m)*r;
        a13=(X_vr+m)*v + 2*X_rr*r;
        a14=0;
        a15=0;
        a16=0;

        a21=(Y_ur-m)*r + Y_uv*v;
        a22=2*Y_vv*abs(v) + Y_uv*u;
        a23=2*Y_rr*abs(r) + (Y_ur-m)*u;
        a24=0;
        a25=0;
        a26=0;

        a31=N_ur*r + N_uv*v;
        a32=2*N_vv*abs(v) + N_uv*u;
        a33=2*N_rr*abs(r) + N_ur*u;
        a34=0;
        a35=0;
        a36=0;

        a41=cos(psi);
        a42=-sin(psi);
        a43=0;
        a44=0;
        a45=0;
        a46=-u*sin(psi) - v*cos(psi);

        a51=sin(psi);
        a52=cos(psi);
        a53=0;
        a54=0;
        a55=0;
        a56=u*cos(psi) - v*sin(psi);

        a61=0;
        a62=0;
        a63=1;
        a64=0;
        a65=0;
        a66=0;

        A_0 = [ a11 a12 a13 a14 a15 a16;
                a21 a22 a23 a24 a25 a26;
```

```

        a31 a32 a33 a34 a35 a36;
        a41 a42 a43 a44 a45 a46;
        a51 a52 a53 a54 a55 a56;
        a61 a62 a63 a64 a65 a66 ];

B_0 = [1      0;
       0      Y_deltar*u^2;
       0      N_deltar*u^2;
       0      0;
       0      0;
       0      0];

A = inv(M)*A_0;
B = inv(M)*B_0;

%-----
% Check the controlability
%-----
C = sqrt(Q);
ctrl=rank([C; C*A; C*A^2; C*A^3; C*A^4; C*A^5]);
if (ctrl < 6)
    fprintf('\nSystem in no longer controllable!!!\n');
    return;
end

%-----
% Compute Control Gains and Control Input
%-----

gain = lqr(A,B,Q,R);

%      K(1,1,ii) = 0;
%      K(1,2,ii) = 0;
%      K(1,3,ii) = 0;
%      K(2,1,ii) = 0;
%      K(2,2,ii) = 0;
gain(2,3) = 0;
gain(2,4) = 0;
gain(2,5) = 0;

else
    gain = K;
end

u_err    = x(1) - x_ref(1); % Surge error
v_err    = x(2) - x_ref(2); % Sway error
r_err    = x(3) - x_ref(3); % Yaw rate error
xpos_err = x(4) - x_ref(4); % x position error
ypos_err = x(5) - x_ref(5); % y position error
psi_err  = x(6) - x_ref(6); % psi (heading) error

while( abs(psi_err) > pi )
    psi_err = psi_err - sign(psi_err)*2*pi;
end

x_err = [u_err;
        v_err;
        r_err;
        xpos_err;
        ypos_err;

```

```

        psi_err];

    if(ii==1)
        deltaU = -gain * x_err;
    else
        deltaU = -K*x_err;
    end

    trust_coeff = .7938; %u=kv^2 --> k = 19.846/25
    Uss = trust_coeff * (speed)^2;
    Uss = 0;

    range_error = sqrt( xpos_err^2 + ypos_err^2 );
    range_gain = 5;

    if(range_error==0)
        range_comp = 0;
    else
        range_comp = range_gain * range_error;
    end

    U_nonlinear(1) = deltaU(1) + Uss + range_comp;

    U_nonlinear(2) = deltaU(2);
    % U_nonlinear = deltaU;

    if( abs(U_nonlinear(2)) > rudder_sat*pi/180 )
        U_nonlinear(2) = rudder_sat*pi/180*sign(U_nonlinear(2));
    end

    if( abs(U_nonlinear(1)) > 19.845 )
        U_nonlinear(1) = 19.845;
    end

    if( U_nonlinear(1) < 0 )
        U_nonlinear(1) = 0;
    end

end

```

## BIBLIOGRAPHY

## BIBLIOGRAPHY

- [1] A.J. Healey and D. Lienard, "Multivariable Sliding Mode Control for Autonomous Diving and Steering of Unmanned Underwater Vehicles," *IEEE Journal of Oceanic Engineering*, Vol. 18, pp 327-339, Jul 1993.
- [2] T. Prestero, "Verification of a Six-Degree of Freedom Simulation Model for the REMUS Autonomous Underwater Vehicle," M.S. Thesis Massachusetts Institute of Technology, Sep 2001.
- [3] L. Fodrea, "Obstacle Avoidance Control for the REMUS Autonomous Underwater Vehicle", Naval Postgraduate School, December 2002.

- [4] Department of the Navy (2004). *The Navy Unmanned Undersea Vehicle (UUV) Master Plan*. 2005
- [5] R. D. Blidberg, “The Development of Autonomous Underwater Vehicles (AUVs); A Brief Summary”, Autonomous Undersea Systems Institute, ICRA, Seoul, Korea, May 2001.
- [6] E. Savage, “Cooperative Control of Autonomous Underwater Vehicles”, Texas A&M University, May 2003.
- [7] J. Keller, “Tracking Control of Autonomous Underwater Vehicles”, Naval Postgraduate School, December 2002.
- [8] J. Grabelle, “Follow the Leader: Formation Control of Multiple Autonomous Underwater Vehicles Using Forward Looking Sonar”, Naval Postgraduate School, June 2005.
- [9] R. K. Lea, R. Allen, and S. L. Merry, “A Comparative Study of Control Techniques for an Underwater Flight Vehicle”, *International Journal of Systems Science*, Vol. 30, Number 9, pp 947-964, August 1998.
- [10] F. Repoulis and E. Papadopoulos, “Planar Trajectory Planning and Tracking Control Design for Underactuated AUVs”, *Elsevier Science Direct*, Vol. 34, pp 1650-1667.
- [11] W. S. Levine, *The Control Handbook*, CRC Press LLC, 1996.
- [12] F. L. Lewis and V. L. Syrmos, *Optimal Control*, Second Edition. John Wiley and Sons, 1995.
- [13] E. Fiorelli, N. E. Leonard, P. Bhatta, and D. Paley, “Multi-AUV Control and Adaptive Sampling in Monterey Bay”, *IEEE Journal of Oceanic Engineering*, Vol. 31, Number 4, pp 935-948, October 2006
- [14] A. Okamoto, J. Feeley, D. Edward, and R. Wall, “Robust control of a Platoon of Underwater Autonomous Vehicles”, *Oceans’04 Techno-Ocean’04 (OTO’04) Conference Proceedings*, pp 505-510.
- [15] A. Okamoto and D. Edwards, “Regulating a Formation of a Large Number of Vehicles”, *Proceedings of the 2005 ASME International mechanical Engineering Congress and Exposition*, Orlando, Florida, November 2005.

- [16] D. Edwards, T. Bean, D. Odell, and M. Anderson, "A Leader-Follower Algorithm for Multiple AUV Formaitons", Proceedings of 2004 IEEE/OES Autonomous Underwater Vehicles, Sebasco Estates, Main, June 2004.
- [17] R. Engel and J. Kalwa, "Coordinated Navigation of Multiple Underwater Vehicles", Proceedings of 2007 International Offshore and Polar Engineering converence, Lisbon, Portugal, July 2007.
- [18] E. Børhaug, A. Pavlov, R. Ghabcheloo, K. Pettersen, A. Pascoal, and C. Silvestre, "Formation Control of Underactuated Marine Vehicles with Communcation Constraints", Proceedings of the 7<sup>th</sup> IFAC Conference on Maneuvering an Control of Marine Craft (MCMC), Lisbon, Portugal, 2006.
- [19] F. Fahimi, "Real Time Trajectory Planning for Groups of Unmanned Vehicles", Final Technical Report, Center of Nonlinear Dynamics and Control, Villanova University, August 2005.
- [20] Sname, The Society of Naval Architects and marine Engineers (1950), "Nomenclature for Treating the Motion of a Submerged Body Through a Fluid", Technical Research Bulletin, No. 1-5, NY, USA.
- [21] X. Xiang, B. Jouvencel, and O. Parodi, "Coordinated Formation Control of Multiple Autonomous Underwater Vehicles for Pipeline Inspection", International Journal of Advanced Robotic Systems, Vol. 7, Number 1, pp 075-084, 2010
- [22] A. E. Bryson and Y. C. Ho, *Applied Optimal Control*, Hemisphere, New Your, 1975.

## **CURRICULUM VITAE**

John Gornowich received a Bachelor of Science in Electrical Engineering with a specialization in Control Systems and a Minor in Business from George Mason University in 2008. He completed his Master of Science in Electrical Engineering from George Mason University in 2010. He started his career with Lockheed Martin MS2 before joining Progeny Systems Corporation in 2009 where he is currently employed.